A study of the intracellular delivery of functional nucleic acids by faint electric treatment

微弱電流処理による機能性核酸の細胞内送達に関する研究

Hasan Mohammad Mahadi
Department of Biophysical Chemistry
Kyoto Pharmaceutical University, Japan
2017

Table of contents

Preface

Effective intracellular delivery of functional nucleic acids remains a significant challenge. To overcome this long standing problem, I have conducted research on *in vitro* iontophoresis or faint electric treatment (fET) mediated intracellular delivery of functional nucleic acids and their underlying mechanism at the department of Biophysical Chemistry of Kyoto Pharmaceutical University. I have found for the first time that fET induced rapid and homogeneous cytoplasmic delivery of functional nucleic acids by activating energy dependent pathways along with the alteration of membrane potential. Furthermore, I have found that fET induced unique endocytosis, of which endosomes can leak macromolecules MW < 10000, and succeeded in the significant regulation of lipid accumulation in adipocytes for application to obesity therapy. This PhD thesis is divided into two chapters. Data of the first chapter have been published at the 'Journal of Controlled Release' while data of the second chapter have been published at the journal of 'Science and Technology of Advanced Materials'. Due to the limitation of time of PhD course, data regarding the fET induced intracellular influx of Ca^{2+}, effect of Ca^{2+} chelator EGTA on fET mediated cellular uptake of siRNA and effect of fET on actin cytoskeleton in chapter I have not yet published. Unpublished data < 30 % have been added to this thesis.

Lastly, I believe my research will make a significant contribution and innovation in the field of drug delivery system.

Abbreviations

ASO	Anti-sense oligonucleotide
B16F1-Luc	B16F1-luciferase expressing cell
CLSM	Confocal laser scanning microscopy
cm	Centimeter
DMEM	Dulbecco's modified Eagle's medium
dSC	2'-Deoxy-4'-thiocytidine
FBS	Fetal bovine serum
fET	Faint electric treatment
FDA	Food and Drug Administration
FITC	Fluorescein isothiocyanate
FNAs	Functional nucleic acids
g/mol	Gram/mole
GFP	Green fluorescence protein
h	Hour
iRed	Intelligent shRNA expression device
ISMB	In-stem molecular beacon
IP	Iontophoresis
LFN	Lipofectamine 2000
Luc	Luciferase
M	Molar
mA	Milliampere
mg	Milligram
min	Minute
miRNA	MicroRNA
ml	Milliliter
mm	Millimeter
mM	Millimolar
mRNA	Messenger RNA

mV	Millivolt
nm	Nanometer
^{o} C	Degree Celsius
PBS	Phosphate buffered saline
PCR	Polymerase chain reaction
pDNA	Plasmid DNA
pmol	Pico mole
RNAi	RNA interference
RES	Reticuloendothelial system
S	Second
SD	Standard deviation
shRNA	Small hairpin RNA
siRNA	Small interfering RNA
SSO	Splice switching oligonucleotide
T3	3,3’,5-Triiodo-L-thyronine
T4	L-thyroxine
TRP	Transient receptor potential
v/v	Volume/volume
µg	Microgram
µl	Microliter
µm	Micrometer
µM	Micromolar
w/v	Weight/volume

Abstract

Effective delivery of macromolecular drugs especially functional nucleic acids into the target cells is important for the therapies of several diseases. However, some inherent properties of cells such as the lipophilic plasma membrane represent a dynamic barrier that restricts entry of extraneous hydrophilic and charged macromolecules into cells. In addition, inefficient endosomal escape is another obstacle to effective delivery of nucleic acids. Iontophoresis is a non-invasive transdermal drug delivery technology, which facilitates transdermal delivery of water soluble and ionized molecules by the application of faint electricity (0.5 mA/cm^2 or less) with electrodes on skin surface. The electric treatment on the skin provides driving force for transdermal delivery of drug molecules. Thus, the application of faint electric treatment (fET) would be a promising candidate for the intracellular delivery of nucleic acids. In this study, I examined the effects of fET on the cellular uptake and cytoplasmic delivery of functional nucleic acids.

I. Faint electric treatment-induced rapid and efficient delivery of nucleic acids into the cytoplasm

RNA interference (RNAi) is the basic endogenous mechanism for regulation of target gene expression in cells activated by small interfering RNA (siRNA). To explore whether fET induces cellular uptake of functional nucleic acids, the RNAi effect from fET of cells stably expressing luciferase in the presence of naked anti-luciferase siRNA was examined. Significant RNAi effect obtained from fET (0.34 mA/cm^2) of cells indicates that fET can deliver naked siRNA into the cytoplasm of cells. Cytoplasmic delivery after fET was analyzed by confocal laser scanning microscopy (CLSM) using an oligonucleotide probe, in-stem molecular beacon (ISMB) that fluoresces upon binding to the complementary mRNA in cytoplasm. Interestingly, ISMB fluorescence appeared rapidly and homogeneously in the cytoplasm of cells when fET of cells expressing luciferase was performed with naked ISMB-luciferase. This result indicates that fET markedly enhances cytoplasmic delivery. In addition, the comparative study of Lipofectamine 2000 (LFN) based delivery of ISMB and fET based delivery of ISMB showed that significant fluorescent intensity was observed in cells with fET even at 15 min and over 4-fold higher fluorescence than that of LFN at 30 min. Moreover, fluorescent signals were observed in all cells treated with fET/ISMB, whereas heterogeneous distribution of fluorescent signals was recognized in the cells after transfection of ISMB/LFN lipoplexes. These results indicate that fET delivered ISMB homogeneously into cytoplasm with faster speed than LFN. Cytotoxicity of fET method was evaluated by trypan blue exclusion test. Cells immediate after fET were not stained by trypan blue dye, indicating that fET did not induce electricity based cytotoxicity such as electroporation, membrane damage, and cell death. Mechanistic study demonstrated that macropinocytosis inhibitor, amiloride, caveolae-mediated endocytosis inhibitor, filipin, and low temperature exposure significantly suppressed fET-mediated cellular uptake of fluorescent-labeled siRNA, indicating that cellular uptake mechanism mediated by fET is endocytosis. In addition, voltage sensitive dye DiBAC4 (3) uptake was increased by fET, suggesting that fET would alter the membrane potential. Moreover, non-specific cationic ion channel such as transient receptor potential channel (TRP) inhibitor SKF96365 reduced uptake of fET-induced fluorescent-labeled siRNA. These results indicate that TRP channels would be involved in

fET based cellular uptake process, in which the alteration of membrane potential occurs via the activation of TRP channel, leading to the cellular uptake of nucleic acids.

II. The novel functional nucleic acid iRed effectively regulates target genes following cytoplasmic delivery by faint electric treatment

Intelligent shRNA expression device (iRed) is a newly synthesized nucleic acid. It contains the minimum essential components needed for shRNA expression in cells such as U6 promoter and shRNA-encoding region, in which any one type of adenine (A), guanine (G), cytosine (C), or thymine (T) nucleotide unit was substituted by each cognate 4'-thio derivatives. iRed is expected as a novel tool for the regulation of target genes. However, general delivery carriers consisting of cationic polymers/lipids could impede function of a newly generated shRNA via electrostatic interaction in the cytoplasm. To overcome difficulties of iRed delivery, I examined the effect of fET on the cells stably expressing luciferase in the presence of iRed encoding anti-luciferase shRNA. Transfection of lipofectamine 2000 (LFN)/iRed lipoplexes showed an RNAi effect, while fET-mediated iRed transfection did not suppress luciferase activity of cells. The difference between siRNA/ISMB and iRed was attributed to their molecular sizes. The observation of intracellular trafficking of different-sized molecules such as FITC-dextran 10,000 and FITC-dextran 70,000 after fET suggested that endosomal escape efficiency of materials internalized by fET depends on the molecular size. Thus, significantly larger molecular size of iRed than siRNA and ISMB is likely to prevent endosomal escape after fET-mediated endocytosis. To improve endosomal escape of iRed taken up by endocytosis, fET with iRed was performed in the presence of chloroquine, which is known as lysosomotropic agent that accumulates in endosomes and lysosomes and enhances cytoplasmic delivery of various compounds. Interestingly, fET in the presence of chloroquine significantly increased the RNAi effect of iRed/fET to levels that were higher than those for the LFN/iRed lipoplexes. Furthermore, the amount of lipid droplets in adipocytes significantly decreased after fET in the presence of chloroquine with iRed against resistin that is a key adipokine of adipocyte maturation. The confocal microscopy of the intracellular trafficking of FITC-labeled iRed showed that green dots (FITC-labeled iRed) co-localized with red dots (endosomes/lysosomes) in the cells after fET without chloroquine, while the green fluorescence was widely distributed in the cells after fET with chloroquine. This indicates that endosomal escape of iRed was significantly increased after fET with chloroquine. Thus, fET of iRed carrying shRNA against resistin in the presence of chloroquine can suppress lipid accumulation during adipocyte maturation, suggesting that a combination of iRed with fET is a useful method for effective regulation of target gene expression.

From these findings, fET can enhance cellular uptake and rapid cytosolic delivery by inducing energy-dependent pathways along with the activation of cationic channels. Thus, faint electric treatment could be useful for effective and safe delivery of functional nucleic acids into the cytoplasm of target cells.

Introduction

Feature of functional nucleic acids (FNAs)

Over the last decade, remarkable progresses have been seen for the development of nucleic acids based therapeutics. Functional nucleic acids (FNAs) are those nucleic acids or their closely related compounds attempt to use them for the treatment of diseases. So far, many FNAs have been developed, such as small interfering RNA (siRNA), short hairpin RNA (shRNA), antisense oligonucleotide (ASO), splice switching oligonucleotide (SSO), plasmid DNA (pDNA), or other DNA based constructs [1, 2]. FNAs are broadly categorized into several sets or groups based on their mechanism of actions in cytoplasm or nucleus [3]. Such as:

- First group consists siRNA, shRNA, and micro RNA (miRNA) that utilize RNAi interference (RNAi) mechanism. After entering into the cytoplasm, these small RNA based FNAs utilize Argonaute containing RISC complexes to degrade their complementary mRNA recognized by Watson-Crick base pairing [1].
- Second group contains ASOs which are 15-30 base pairs DNA, RNA or their closely related constructs. Upon delivery into cytoplasm or nucleus, ASOs recognize their target mRNA by Watson-Crick base pairing and cleave them via RNAase H dependent mechanism or interact with pre-mRNA during the splicing process [4].
- Group three consists a special group of oligonucleotides called aptamer that have the ability to act as ligands for proteins, often for receptors in either the intracellular or extracellular environment to affect their functionality. Aptamers are single stranded synthetic DNA or RNA and usually 56-120 nucleotides long [5].
- Group four consists pDNA or other DNA constructs. Delivery of these FNAs to the nucleus inducing subsequent expression of a transgene [3].

Upon binding to the intracellular targets, FNAs regulate gene expression to inhibit the production of abnormal proteins related to disease or replace abnormal and non-functional proteins related to the disease by transgene expression.

Recognition of FNAs as drug

After extensive research studies and clinical trials some FNAs are approved as drug for the treatment of diseases [2, 6]. So far, four ASOs and one aptamer drug are approved by Food and Drug Administration (FDA) of USA (Table 1). Like USA, Chinese Food and Drug Administration and European Union each approved one FNA based drug for the treatment of disease (Table 1). Except these approved drugs, a numbers of FNAs are remained in clinical trials or await for approval.

Table 1. Summary of FNAs approved as drug.

Name of Drug	Types of FNAs	Target	Disease condition	Approved country
Fomivirsen	ASO	IE2	Cytomegalo retinitis	USA (1998)
Mipomersen	ASO	ApoB 100	Hypercholesterolemia	USA (2013)
Eteplirsen	ASO	Exon 51	Duchenne muscular dystrophy	USA (2016)
Nusinersen	ASO	SMN2	Spinal muscular atrophy	USA (2016)
Pegaptanib	Aptamer	VEGF165	Age related muscular degeneration	USA (2004)
Gendicine	Recombinant adeno-vector	Express p53 gene	Squamous cell carcinoma	China (2003)
Alipgene	Recombinant adeno-associated vector	Express lipase gene	Lipoprotein lipase deficiency	European Union (2012)

Challenges for FNAs drug

For effective regulation of target gene expression as well as for effective therapy, FNAs must be needed to reach their intracellular site such as cytoplasm or nucleus of the target cell. Thus, the functionality of FNAs largely depends on their effective delivery. However, delivery of FNAs to their targeted site remains a major challenge due to the presence some inherent biological barriers [7]. These barriers are divided into two parts: such as- extracellular barriers and intracellular barriers. Extracellular barriers of FNAs are extended from their administration to target cell surface. In this route, serum inactivation, enzymatic degradation, reticuloendothelial system (RES) recognition, vascular endothelial layer act as barriers for FNAs [1]. However, extracellular barriers usually depend on the route of administration. Additionally, modification of nucleic acids, such as backbone modifications increases nuclease resistance while sugar modification may decrease immunogenicity, improve stability and bioavailability of FNAs [8]. Thus, depending on the route of administration and chemical evolution, FNAs are expected to overcome extracellular barriers [3]. In the present study, I focus on intracellular delivery of FNAs.

Intracellular barriers for delivery of FNAs

Most prominent cellular barriers that restrict the entry of FNAs into their targeted site are recognized as plasma membrane and endosomal entrapment [9]. The plasma membrane of living cells is a dynamic structure that is lipophilic in nature. As a result, it deprives the entry of hydrophilic, charged and large sized molecules. In a physiochemical manner, FNAs are high molecular sized and negatively charged molecules.

Thus, plasma membrane makes it difficult for FNAs to enter into cells by electrostatic repulsion [9]. Moreover, no trans-membrane receptors for FNAs are present in the plasma membrane to activate cellular uptake process. As a result, disruption of plasma membrane or any assistance of carriers is needed to overcome the plasma membrane barrier.

The endocytosis pathway is the fundamental cellular uptake mechanism of cells for macromolecules, virus and pathogens. This pathway composed of vesicle known as endosome which mature in a unidirectional manner from early endosome to late endosome before fuse with intracellular organelles called lysosomes [10]. After internalization of extraneous molecules via endocytosis, molecules remain in endosome and there is no access of these molecules into cytoplasm or nucleus. Therefore, escape from endosome is essential step for efficient delivery of FNAs into their intracellular sites. A quantitative study reveals that very small fraction of FNAs (1-2%) release from endosomes from carrier based delivery [11]. Due to the inefficient endosomal escape, FNAs remain for longer period of time into endosomes which reduces their functionality as well as increases the susceptibility of their degradation by nuclease.

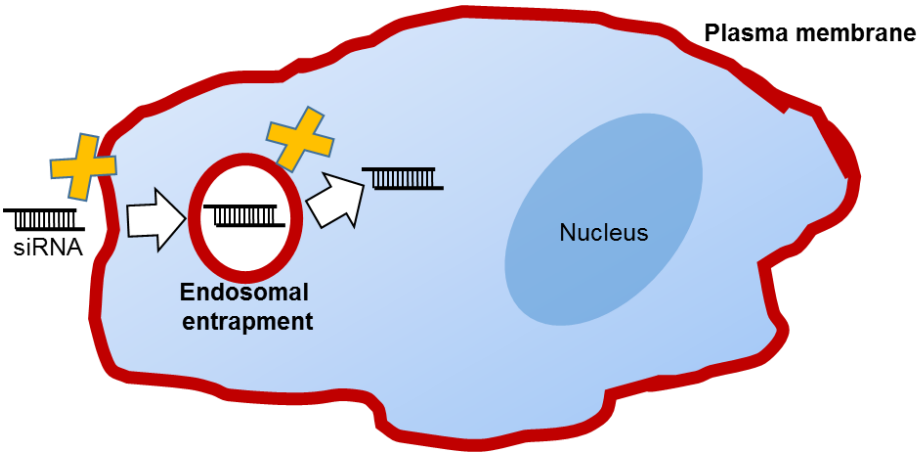

Figure 1. Plasma membrane and endosomal entrapment represent significant cellular barriers for intracellular delivery of FNAs.

Except these cellular barriers, some physiochemical properties of FNAs such as high molecular size, negatively charged, low lipophilicity, and low stability in biological environment make their delivery and translocation to the active cellular compartments more complex.

Approaches for intracellular delivery of FNAs

To overcome these existing barriers for intracellular delivery of FNAs upon considering their physiochemical properties, huge research studies have been performed over the last decades. So far, a wide range of intracellular delivery systems have been reported [12, 13]. Based on the mechanism of delivery, these delivery systems are broadly categorized into two groups, such as membrane disruption mediated delivery system and carrier mediated delivery system [14]. Membrane disruption based system is mostly physically facilitated method. This system delivers FNAs upon disrupting the membrane via

permeabilization or direct penetration. Thermal, electrical, optical, mechanical, or other types of physical forces are used to explore the delivery of FNAs in membrane disruption mediated system. These physical forces deliver cargoes remain dispersed in solution [14]. This delivery method is suitable for a wide range of cell types and also can be used in combination with non-viral carrier mediated method.

The contrary to the membrane disruption mediated method, carrier based delivery system uses cellular uptake process of endocytosis to deliver the cargo into cells. Lipid/polymer/inorganic nanocarriers, viral vectors, exosome, vesicles, and cell penetrating peptides etc. are used to deliver FNAs into cells in carrier based delivery system [15, 16]. In this system, carriers interact with FNAs and usually package them into condensed form to protect FNAs. After packing, carriers bring FNAs into cells upon using cellular uptake process such as endocytosis [11]. The activation of cellular uptake pathways generally depends on the interaction of carriers and cell surface or physiochemical properties of carriers [17]. After taken up the cargo by endocytosis, they need to escape from endosome during the endosomal progression such as from early endosome to late endosome or before fuse with lysosome to reach their intracellular sites [10]. Therefore, carrier mediated delivery systems package FNAs and release them at the targeted site using cellular uptake and membrane trafficking mechanism of cells.

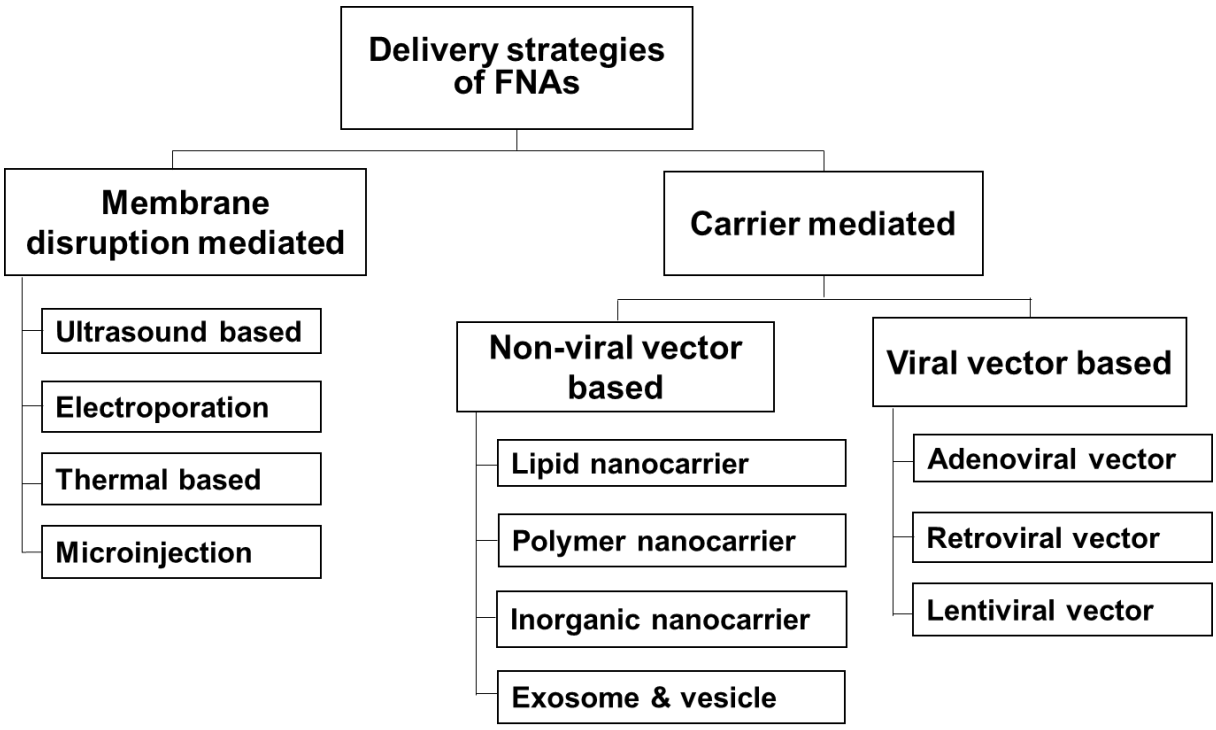

Figure 2. An overview of intracellular delivery systems for FNAs.

Challenges of intracellular delivery methods for FNAs

To overcome the fundamental challenges of intracellular delivery of FNAs, the versatile applications of these above delivery systems remained still unsatisfactory due to some undesirable issues of delivery

efficiency and cytotoxicity of the delivery systems [18, 19]. Although membrane disruption method is applicable for wide ranges of cell types, but common problems of this method are induction of plasma membrane injury and excessive cell damage. Additionally, the level of cell damage varies from cells to cells, so it is difficult to optimize their application for effective delivery of FNAs [14]. Moreover, this method also causes the loss of cytoplasmic contents, excessive damage of organic molecules, protein denaturation and internal membrane breakdown due to the application of physical forces [20]. Furthermore, some of these physical methods are not suitable for *in vivo* translation.

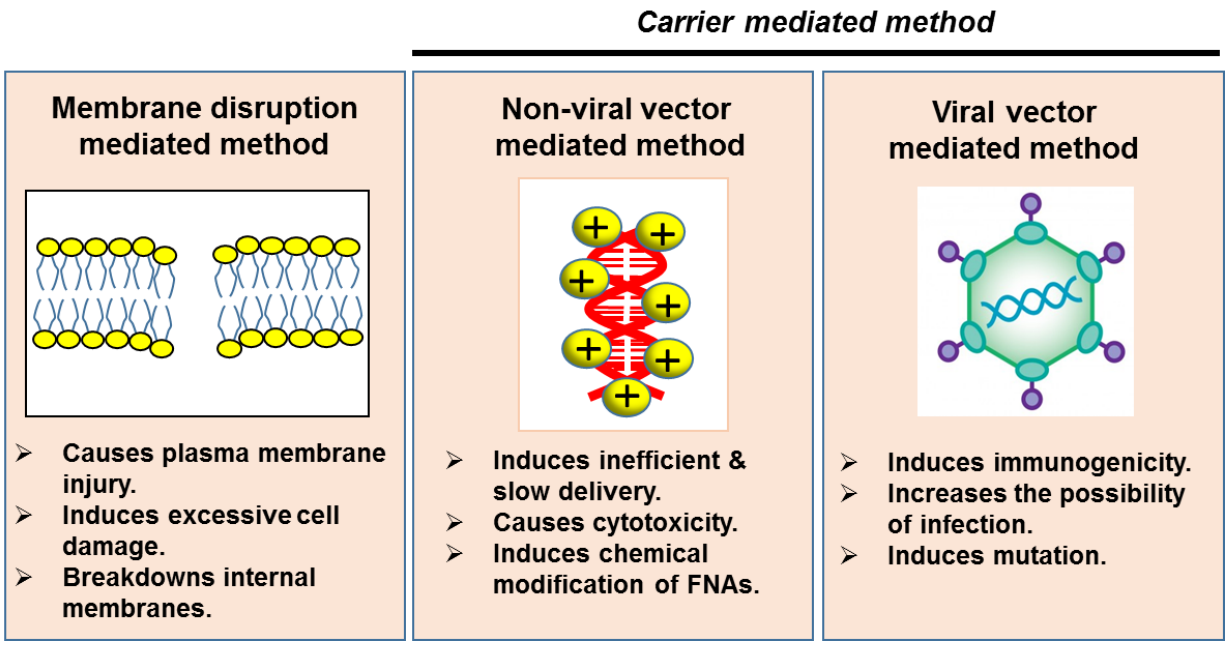

Figure 3. Drawbacks of intracellular delivery systems for FNAs.

On the other hand, the successful outcome from carrier based delivery of FNAs depends on many factors. In case of non-viral mediated method, the physiochemical properties of carriers such as shape, size, charge and hydrophobicity of carriers are important. Additionally, some properties of cells such as having receptor for carriers, uptake activity of cells, and endosomal escape are also important issues [17]. However, non-viral vector mediated delivery method is slow and their delivery efficiency is low due to the inadequate endosomal escape [11]. Moreover, induction of cytotoxicity from carrier materials and chemical modifications of FNAs by carriers are also common claims for non-viral vector based methods [18]. On the contrary of non-viral mediated method, viral vectors can deliver FNAs rapidly and effectively into cells but they are associated with the induction of host immune response and increase in the possibility of infection [21]. Due to the infective delivery efficiency and toxicity of carriers, effective intracellular delivery of FNAs still remains a significant challenge. Therefore, more safe and sophisticated intracellular delivery technology of FNAs is needed. To overcome these long standing drawbacks behind the intracellular delivery of FNAs, in this study, I focus on faint electric treatment (fET) or *in vitro* iontophoresis.

Iontophoresis (IP) is a non-invasive transdermal drug delivery technology

Iontophoresis (IP) has recently attracted the attention of researchers studying drug delivery systems. It is a promising non-invasive transdermal drug delivery technology [22, 23, 24]. IP facilitates transdermal delivery of water soluble and ionized molecules by the application of faint electricity with electrodes on skin surface. Density of electricity used in IP is 0.5 mA/cm^2 or less [25]. The electric treatment on the skin provides driving force for transdermal delivery of drug molecules into the skin.

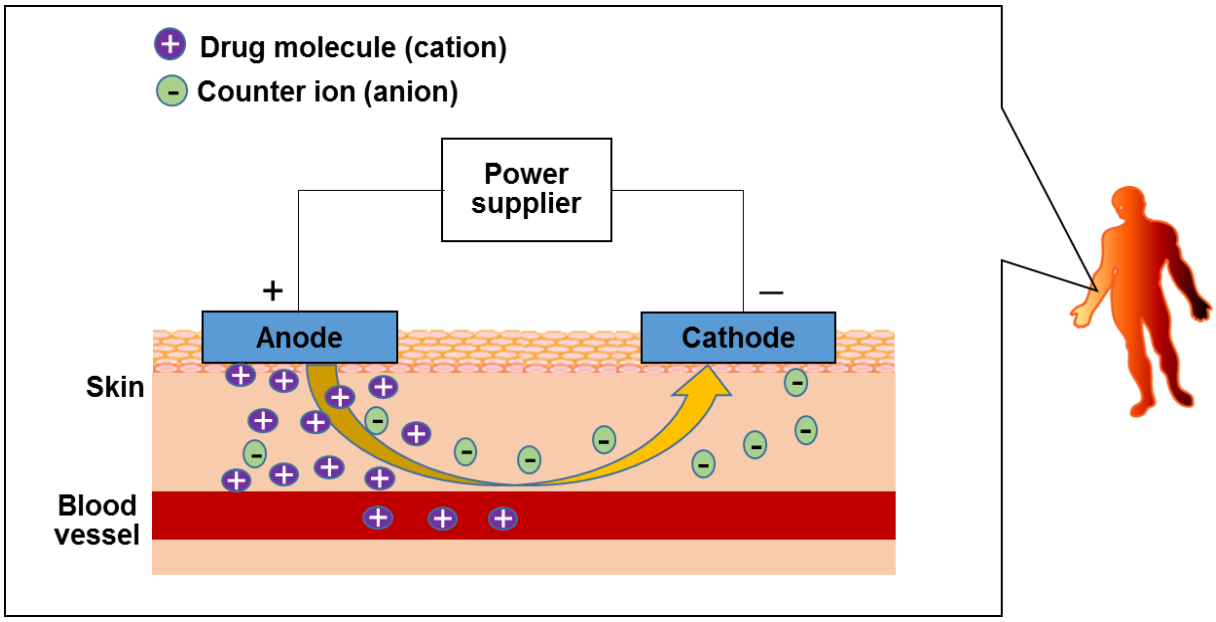

Figure 4. Transdermal drug delivery by IP. IP electrodes- the anode and the cathode (blue color) are placed on the skin surface. Violet colored positively charged molecules indicate as drugs while negatively charged molecules indicate as counter ions remained in the reservoir under the same charged electrode before IP. During application, the faint electricity of IP delivers drug molecules into the skin.

Moreover, IP can deliver charged nanostructures, such as liposomes and nucleic acids into skin [26, 27, 28, 29]. A mechanistic study of this transdermal penetration of liposomes revealed that faint electricity of iontophoresis dissociates intracellular junctions via activation of cell signaling pathway [29]. It has been previously reported that IP induces *in vivo* non-invasive transdermal delivery of functional nucleic acid siRNA and shows significant RNAi effect [26]. But, how *in vivo* IP of siRNA induces RNAi effect and whether the faint electricity of IP induces cellular uptake or intracellular delivery of FNAs still remain unclear. As *in vivo* IP non-invasively induces transdermal delivery of siRNA, the application of faint electric treatment (fET) would be a promising candidate to study intracellular delivery of FNAs. fET induces the physiological changes for the effective delivery of liposomes. Inflow of calcium ions into cells is activated by fET with liposomes [29], possibly followed by the alteration of membrane potential.

Cells possess membrane potential that refers to the voltage difference across the plasma membrane that is established by the balance of intracellular and extracellular ionic concentrations and maintained via passive and active transport of ions through various ion channels within plasma membrane [30]. In addition, alteration of membrane potential changes cellular physiology and can initiate cellular uptake process during depolarization condition [31]. To examine the application of faint electricity for intracellular delivery of FNAs, in the present study I hypothesize that, fET would induce cellular uptake and cytoplasmic delivery of FNAs by changing cellular physiology. Based on the hypothesis, herein, I examined the effect of fET on cellular uptake and cytoplasmic delivery of FNAs. In chapter I, I evaluated the effect of fET on cellular uptake of siRNA, and analyzed cytoplasmic delivery and cellular uptake mechanism. In chapter II, I examined the intracellular delivery of a novel functional nucleic acid intelligent shRNA expression device (iRed) to evaluate the possible use of fET based delivery of FNAs.

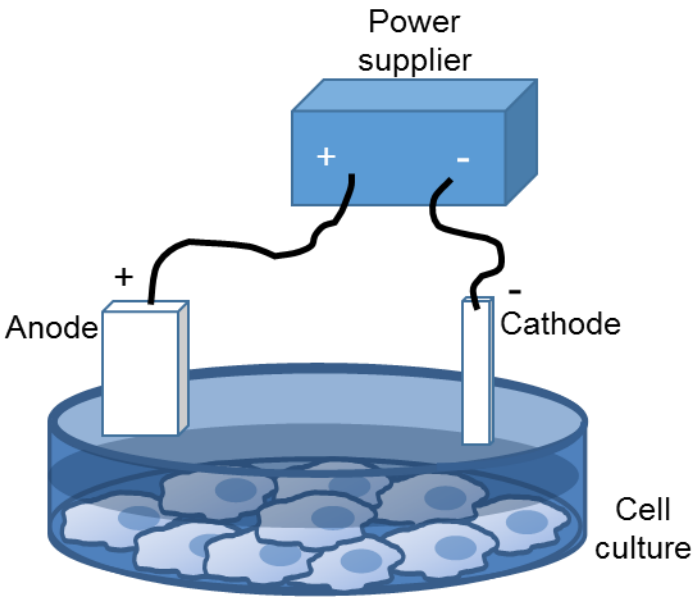

Figure 5. Schematic representation of fET of cells. Cells are seeded on 35 mm dish. After 18 h of cultivation, cells are washed with PBS and add serum free medium containing desired macromolecules or reagents. Ag-AgCl electrodes with 2.5 cm^2 surface area are placed into the dish, and cells are treated with a constant current of 0.34 mA/cm^2 for 15 min.

Chapter I. Faint electric treatment induced rapid and efficient delivery of nucleic acids into the cytoplasm.

In the present chapter, I monitored the cellular uptake and cytoplasmic delivery of functional nucleic acids to analyze their underlying mechanisms. RNAi is the fundamental endogenous mechanism for regulation of targeted gene expression in cells induced by siRNA [1]. To explore whether fET induces cellular uptake and cytoplasmic delivery, RNAi effect from fET of cells stably expressing luciferase in the presence of anti-luciferase siRNA was examined. In addition, cytoplasmic delivery after fET was analyzed by CLSM using an oligonucleotide probe known as in-stem molecular beacon (ISMB) which fluoresces upon binding to the target mRNA in the cytoplasm of cells [32]. Moreover, advantages of fET-based delivery were evaluated by the comparative study of fET-based delivery of ISMB with conventional LFN-based delivery of ISMB. The cytotoxicity of fET-based delivery was inspected by trypan blue exclusion test [33]. Fluorescent-labeled siRNA was used for mechanistic study. The effect of low temperature exposure and endocytosis inhibitors such as the macropinocytosis inhibitor, amiloride [34], the clathrin-mediated endocytosis inhibitor, hypertonic sucrose [35], and the caveolae-mediated endocytosis inhibitor, filipin [36] on cellular uptake of fluorescent-labeled siRNA was evaluated to know the uptake mechanism. Additionally, the effect of fET on membrane potential was analyzed using voltage sensitive dye DiBAC4(3) which enter into cells in response to change of membrane potential [37]. Furthermore, the involvement of non-specific cationic ion channels such as TRP channels was evaluated by assessing the effect of TRP channel blocker SKF96365 [38] on cellular uptake of fluorescent-labeled siRNA.

1 Materials and methods

1-1 Cell culture

The mouse melanoma cell line B16F1 was purchased from Dainippon Sumitomo Pharma Biomedical Co, Ltd. (Osaka, Japan). The B16 F1-Luc expressing luciferase, a stable transformants of B16F1 cells was established in our laboratory [39]. B16F1-Luc cells were cultivated in Dulbecco's modified Eagle's medium (DMEM) supplemented with 10% fetal bovine serum (FBS) at 37 ^{o}C in 5% CO_2.

1-2 Materials

Anti-luciferase siRNA (21-mer, 5'-GCGCUGCUGGUGCCAACCCTT-3', 5'-GGGUUGGCACCAGCAGCGCTT-3': anti-Luc) and anti-GFP siRNA (21-mer, 5'-GCUGACCCUGAAGUUCAUCTT-3', 5'-GAUGAACUUCAGGGUCAGCTT-3': anti-GFP), Rhodamine-labeled anti-GFP siRNA (21-mer, 5'-GCUGACCCUGAAGUUCAUCTT-3', 5'-GAUGAACUUCAGGGUCAGCTT-3'), and Lipofectamine 2000 were obtained from Invitrogen Life Technologies (Carlsbad, CA, U.S.A). ISMB against luciferase (5'-C(Cy3:YD)TGG(YD)GTTGGCACCAGCAGCGCAC(Nitromethylred:Nm)(Nm)CCA(Nm)(Nm)G -3':

ISMB-Luc) and ISMB against GFP (5'-G(YD)GTT(YD)GAAGAAGATGGTGCGCTCTC(Nm)(Nm)AAC(Nm)(Nm)C-3': ISMB-GFP) were synthesized by Tsukuba Oligo Service, Inc. (Tsukuba, Japan). Amiloride hydrochloride hydrate and Filipin were purchased from Sigma-Aldrich, Inc. (St. Louis, MO, USA). DiBAC4(3), EGTA, and Fluo-4 calcium kit were purchased from Dojindo Molecular Technologies, Inc. (Rockville, MD, USA). SKF96365, Trypan blue, and sucrose were obtained from Wako Pure Chemical Industries, Ltd. (Osaka, Japan). Rhodamine phalloidin was purchased from Cytoskeleton, Inc. (Denvar, CO, USA). Cell lysis buffer and luciferase assay substrate were purchased from Promega Corporation (Madison, WI, USA). BCA protein assay kit was purchased from Thermo Scientific (Waltham, MA). Ag-AgCl electrode was purchased from 3M Health Care (Minneapolis, MN, USA).

1-3 Faint electric treatment (fET) of cells

For the application of *in vitro* fET, cells were seeded on 35 mm dishes. The number of cells used is indicated in each section bellow. After 18 h of seeding, cells were washed with phosphate buffered saline (PBS), followed by addition of 1 ml serum free DMEM containing 100 pmol anti-Luc siRNA, 100 pmol anti-GFP siRNA, 0.5 μg ISMB-Luc, 0.5 μg ISMB-GFP or 100 pmol rhodamine-labeled siRNA to cells. Then, Ag-AgCl electrodes with 2.5 cm^2 surface area were placed into the dish, and cells were treated with a constant current of 0.34 mA/cm^2 for 15 min.

1-4 Transfection and measurement of luciferase activity

B16F1-Luc cells at a density of $1x10^4$ cells were seeded on 35 mm culture dishes. After 18 h of seeding, cells were washed with PBS and added 1 ml serum free DMEM containing 100 pmol anti-luciferase/ anti-GFP siRNA. Then, fET of cells was performed as describe above. After 3 h of fET, 1 ml DMEM containing 10% FBS was added to the dish and cells were continue to incubate for 45 h. After the incubation, cells were washed with PBS and lysed with reporter lysis buffer according to the manufacturer's protocols. The luciferase assay substrate was added to cell lysate and chemiluminescence intensity was measured by a luminometer (Lumnescensor-PSN, ATTO Corp., Tokyo, Japan). The total protein concentration was measured with BCA protein assay kit according to the manufacturer's protocols.

1-5 Analysis of cytoplasmic delivery by CLSM observation of cells after fET

For evaluation of cytoplasmic delivery, $5x10^4$ cells were cultivated on 0.002% poly-L-lysine coated 35 mm glass bottom dishes. After 18 h of cultivation, cells were washed with PBS and 1 ml serum free DMEM containing 0.5 μg of ISMB-Luc or ISMB-GFP were added to cells. After fET, cells were incubated for 1 h at 37 °C in 5% CO_2. After incubation, cells were observed with CLSM A1R+ (Nikon Co, Ltd., Japan). For time elapse imaging, observation was started immediately after fET of cells.

1-6 Comparison of fET based delivery of ISMB with LFN based delivery of ISMB

For the comparison of fET based delivery with LFN based delivery of ISMB-Luc, B16F1 cells at a density of $5x10^4$ cells were seeded on 35 mm culture dishes. After 18 h of cultivation, cells were washed with PBS. For fET, 800 µl of serum free DMEM containing 0.5 µg ISMB-Luc was added to the dish. For LFN treatment, 800 µl of serum free DMEM containing ISMB-Luc/LFN lipoplex prepared with 0.5 µg ISMB-Luc and 1 µl LFN (according to the manufacture's guidelines) was added to the dish. After fET (15 min, 0.34 mA/cm^2) with ISMB-Luc or addition of LFN/ISMB-Luc lipoplex at various time points such as 15 min, 30 min, and 1 h from the starting point of fET or addition of LFN/ISMB-Luc lipoplex, cells were washed with PBS and lysed with reporter lysis buffer according to the manufacturer's protocols. The fluorescence intensity of cell lysate was measured by a micro plate reader Infinite 200 (Tecan Group Ltd., Mannedorf, Switzerland) at excitation and emission wavelengths of 525 nm and 580 nm, respectively. Regarding CLSM observation, after fET (15 min, 0.34 mA/cm^2) with ISMB-Luc or addition of LFN/ISMB-Luc lipoplex, cells were washed with PBS and observed under CLSM at 30 min or 1 h time points from the starting point of fET of addition of LFN/ISMB-Luc lipoplex.

1-7 Cytotoxicity assay of fET treated cells

For evaluation of electricity induced cytotoxicity, $4x10^5$ cells were seeded on 35 mm culture dishes. After 18 h of cultivation, cells were washed with PBS and 1 ml of serum free DMEM was added into the dish. Then fET (15 min, 0.34 mA/cm^2) was performed. Cells were collected immediately after fET by trypsin treatment and 10 µl of cell suspension was taken into a micro tube. An equal volume, 10 µl of 0.4% trypan blue was added to the cell following incubation of the mixture for 2 min to stained cells. Then the number of stained and non-stained cells were counted. The percentage of cell viability was calculated by the following formula:
The percentage of viability = (100 x number of non-stained cells / total number of cells).

1-8 Treatment with pharmacological inhibitors or low temperature with measurement of fluorescence intensity

For study of cellular uptake mechanism, $1x10^5$ cells were seeded on 35 mm culture dishes. For pharmacological inhibitory experiments, 1 ml of serum free DMEM containing either 0.45 M sucrose, 1 mM amiloride, 5 µg/ml filipin or 25 µM SKF96365 was added to the dish, followed by incubation for 15 min. After the incubation, 100 pmol rhodamine-labeled siRNA was added to the dish and fET (15 min, 0.34 mA/cm^2) of cells was performed. After fET, cells were incubated for 1 h at 37 ^{o}C. For low temperature exposure, 1 ml of serum free DMEM containing 100 pmol rhodamine-labeled siRNA was added into the dish and fET was performed on ice. After incubation, cells were then washed with PBS and lysed with reporter lysis buffer (Promega) according to the manufacturer's protocols. The fluorescence intensity of cell lysate was measured with a microplate reader Infinite 200 (Tecan Group Ltd., Mannedorf, Switzerland) at excitation and emission wavelengths of 546 and 590 nm, respectively.

1-9 Evaluation of intracellular inflow of Ca^{2+} after fET

For Ca^{2+} imaging, $0.5x10^5$ cells were seeded on 0.002 % poly-L-lysine coated 35 mm glass bottom dishes. After 18 h of cultivation, cells were washed with PBS. Then, 1 ml of loading buffer (prepared according to the manufacturer's protocol) was added into the dish and incubated for 1 h at 37° C. In case of EGTA treatment, cells were pre-treated for 30 min with 5 mM EGTA in serum free DMEM medium. After incubation, loading buffer was removed, and 1 ml pre-warmed recording medium (prepared according to the manufacturer's protocols) or medium containing 100 pmol anti-Luc siRNA was added into the dish, followed by fET (0.34 mA/cm^2, 2 min). Immediately after fET, fluorescence signals corresponding to the intracellular Ca^{2+} were observed under CLSM A1R+ (Nikon Co. Ltd. Japan). For evaluation of the effect of Ca^{2+} chelation on fET mediated cellular uptake, $1x10^5$ cells were seeded on 35 mm culture dishes. After 18 h of cultivation, cells were washed with PBS, 1 ml serum free medium containing 5 mM EGTA was added. After incubation for 30 min, 100 pmol rhodamine-labeled siRNA was added to the dish, followed by fET (0.34 mA/cm^2, 15 min). Fluorescence intensity was measured according to the section 1-8.

1-10 Actin staining of cells after fET

For actin staining, $0.5x10^5$ cells were seeded on 0.002 % poly-L-lysine coated 35 mm glass bottom dishes. After 18 h of cultivation, cells were washed with PBS and 1 ml serum free DMEM or DMEM containing 100 pmol anti-luciferase siRNA was added before cells were treated with electricity as described above. Immediately after fET, cells were washed with PBS and fixed with PBS containing 4% para formaldehyde for 10 min at room temperature. After fixation, cells were washed with PBS and were permeabilized by PBS containing 1% triton X-100 for 10 min at room temperature. Cells were then incubated with rhodamine phalloidin at the final concentration of 100 nM for 30 min in dark. After washing, cells were mounted in VECTASHIELD with DAPI and were observed under CLSM A1R+ (Nikon Co. Ltd. Japan).

1-11 Measurement of membrane potential after fET

For the measurement of membrane potential, $5x10^4$ cells were seeded on 35 mm culture dishes. After 18 h of seeding, cells were washed with PBS and added 2 ml of serum free DMEM containing 5 μM DiBAC4(3) dye, followed by incubation for 30 min at room temperature. After the incubation, cells were treated with fET (15 min, 0.34 mA/cm^2). For low temperature exposure, fET was performed on ice. After fET, cells were washed and lysed with reporter lysis buffer (Promega) according to the manufacturer's protocols. The fluorescence intensity of cell lysate was measured using microplate reader Infinite 200 (Tecan Group Ltd., Mannedorf, Switzerland) at excitation and emission wavelengths of 488 and 525 nm, respectively.

1-12 Statistical analysis

Statistical analysis was performed using one-way ANOVA followed by Turkey-Kramer HSD test. *p* values <0.05 were considered to be significant.

2 Results

2-1 Effect of fET on luciferase expression of cells in the presence of naked anti-luciferase siRNA

To determine whether fET induces cellular uptake of functional nucleic acids, the RNAi effect from fET of B16F1-Luc cells stably expressing luciferase in the presence of naked anti-luciferase siRNA was inspected. The luciferase activity of B16F1-Luc cells was significantly suppressed by fET with anti-luciferase siRNA, although the positive control cells incubated with LFN/anti-luciferase siRNA lipoplex showed higher RNAi effect (Figure 6). Regarding the fET of B16F1 cells stably expressing luciferase with anti-GFP siRNA, the suppression effect of luciferase activity was not observed, indicating that the suppression effect was specific for anti-Luc siRNA (Figure 6). This result suggests that fET induced cellular uptake of siRNA into the cytoplasm of cells without the need for any modification of siRNA or other functional devices.

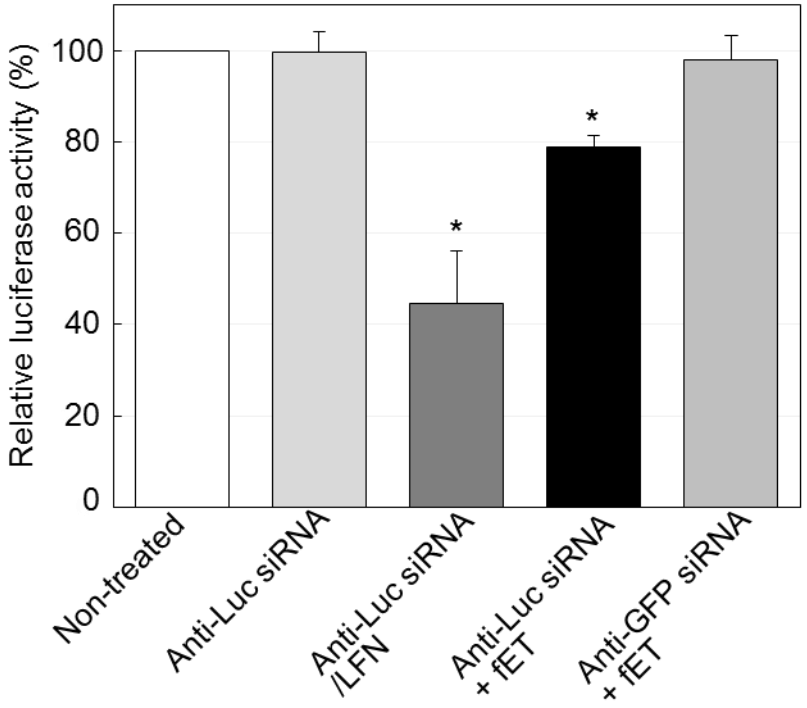

Figure 6. Effect of *in vitro* fET with anti-luciferase siRNA on luciferase activity of B16F1-Luc cells. After 48 h of fET (0.34 mA/cm^2, 15 min) in the presence of naked siRNA, the luciferase activity of cells expressing luciferase was measured. LFN/anti-luciferase siRNA lipoplex was used as a positive control. Data were obtained by three separate experiments, and are expressed as mean ± SD. *p<0.05.
J. Control. Release, 2016, 228, 20-25, Figure 1.

2-2 Evaluation of cytoplasmic delivery process induced by fET

After fET mediated cellular uptake, siRNA induces RNAi effect indicating siRNA must overcome membrane barriers, such as plasma membrane and endosomal membrane to reach cytoplasm. To analyze cytoplasmic delivery process after fET induced cellular uptake, cytoplasmic delivery of an oligonucleotide probe, in-stem molecular beacon (ISMB) was evaluated. The ISMB is an oligonucleotide probe having hairpin shaped structure that contains fluorophores and quenchers. In the absence of complementary mRNA, the fluorescence emission of ISMB is quenched by the interaction between fluorophores and quenchers. On the other hand, in the presence of complementary mRNA, the hairpin structure of ISMB is opened resulting that the fluorophores is released to emit fluorescence [32]. After 1 h of fET, all B16F1-Luc cells showed potent red fluorescence in the present of ISMB-luciferase (ISMB-Luc) while no fluorescence signals were observed from B16F1-Luc cells without fET even in the presence of ISMB-Luc (Figure 7). On the other hand, no fluorescence signal was seen after 1 h of fET of B16F1-Luc cell in the presence of ISMB against GFP (ISMB-GFP). These results suggest that ISMB-Luc efficiently delivers into the cytoplasm after fET induced cellular uptake and specifically binds with target luciferase mRNA into cytoplasm.

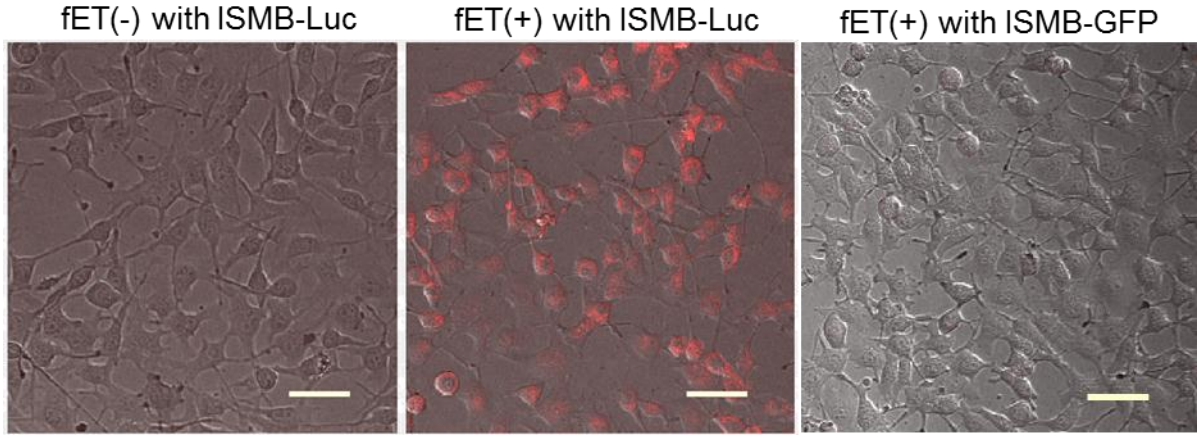

Figure 7. fET-induced cytoplasmic delivery of ISMB. B16F1-Luc cells were treated with fET (0.34 mA/cm^2, 15 min) in the presence of ISMB solutions. Cells were observed with CLSM 1 h after fET. Middle and left panel images were obtained from cells incubated with ISMB-Luc with or without fET. On the other hand, right panel image was obtained from cells incubated with ISMB-GFP in the presence of fET. Red fluorescence signals show cytoplasmic delivery and the association of ISMB with its targeted mRNA. Scale bars indicate 50 μm. ***J. Control. Release, 2016, 228, 20*-25, *Figure 5.***

To analyze cytoplasmic delivery process, in the next step, time-lapse imaging of B16F1-Luc cell in the presence of ISMB-Luc was performed. Surprisingly, immediately after fET, ISMB fluorescence signals appeared in the cytoplasm of the cells. In addition, fluorescence signal intensities were rapidly increased with time for 15 min (Figure 8). On the other hand, even after 15 min, fluorescence signal was not observed in cells with ISMB-Luc without fET (Figure 8). This result suggests that cytoplasmic delivery of functional nucleic acids after fET was very rapid and effective.

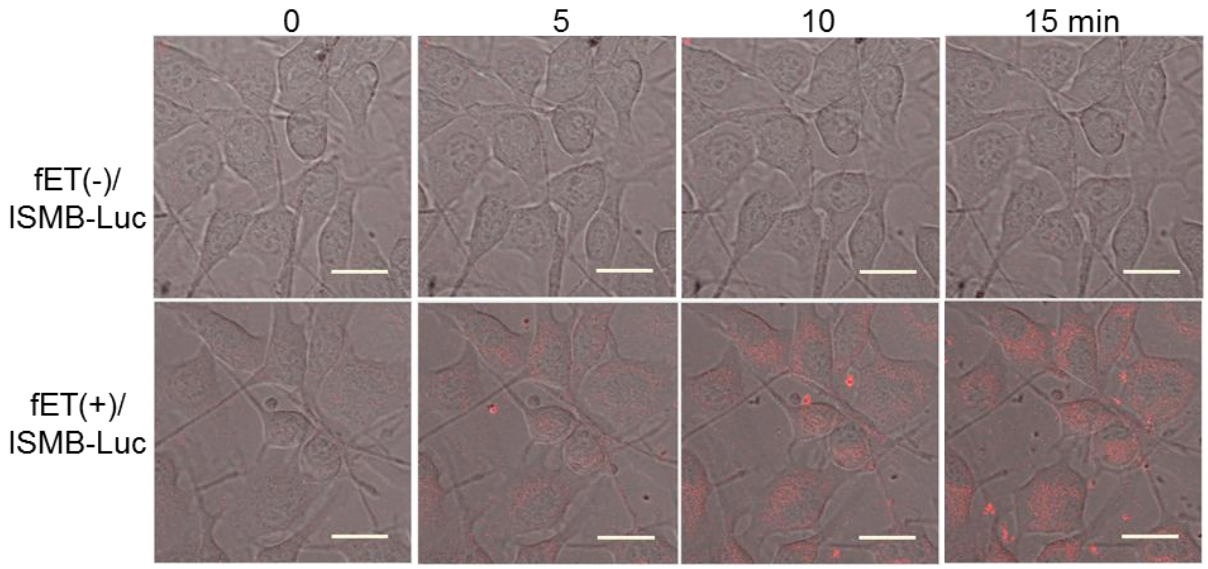

Figure 8. Time-elapse observation of fET-mediated cytoplasmic delivery of ISMB-Luc. In the presence of ISMB-Luc solution, B16F1-Luc cells were treated with fET (0.34 mA/cm^2, 15 min) and time-elapse images were taken immediately after fET at 5 min intervals until 15 min. Red fluorescence signals show cytoplasmic delivery and the association of ISMB with its targeted mRNA. Scale bars indicate 20 μm. ***J. Control. Release, 2016, 228, 20*-25, *Supplemental Figure 2.***

2-3 Comparison study of fET based delivery of ISMB-Luc with LFN based delivery of ISMB-Luc

To evaluate the advantages of fET-based delivery method, fluorescence intensities of B16F1-Luc cells treated with fET (0.34 mA/cm^2, 15 min) in the presence of ISMB-Luc at various time points were compared with cells treated with LFN/ISMB-Luc lipoplex. As a result, significant fluorescence intensity was found in cells treated with fET in the presence of ISMB-Luc even at 15 min. In addition, the fluorescence intensity of fET/ISMB-Luc treated cells was over 4-fold higher than that of LFN/ISMB-Luc treated cells (Figure 9). Furthermore, after fET of cells with ISMB-Luc or transfection of cells by LFN/ISMB-Luc their fluorescence was examined. As a result, red fluorescence signals were observed from all cells treated with fET while heterogeneous distribution of red fluorescence signals was observed after transfection of LFN/ISMB-Luc lipolpex (Figure 10).

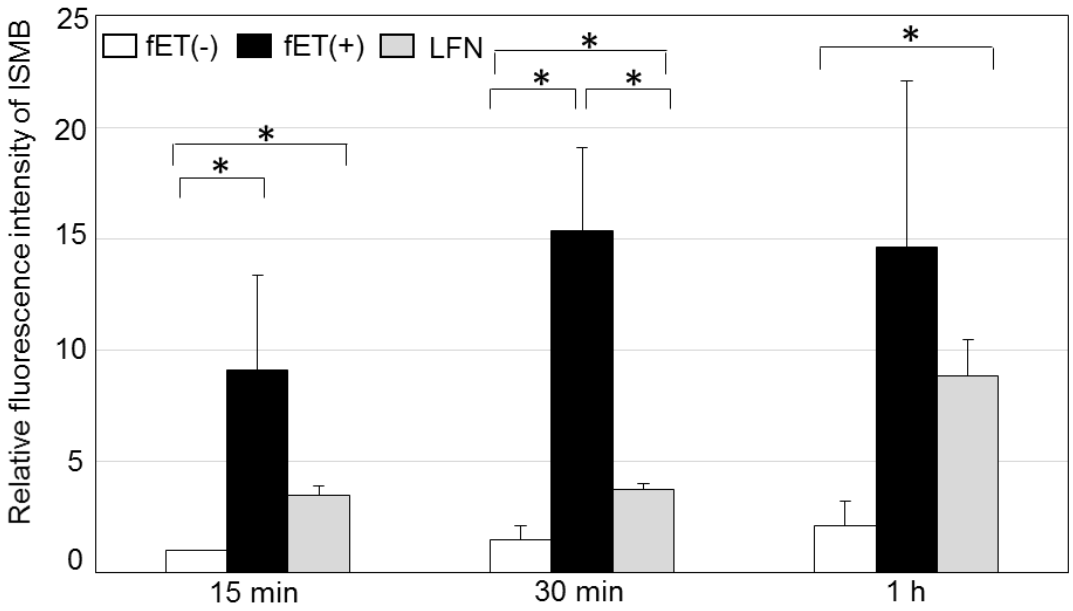

Figure 9. Time-dependent change of fluorescence intensity of ISMB-Luc delivered into cytoplasm. Cells were treated with faint electricity (0.34 mA/cm^2, 15 min) in the presence of ISMB solution or LFN/ISMB lipoplex. After 15 min, 30 min, and 1 h from the start of fET or LFN treatment, fluorescence intensity of the cells was measured. Data were obtained by three separate experiments, and are expressed as mean ± SD. *$p < 0.05$. ***J. Control. Release, 2016, 228, 20-25, Supplemental Figure 3.***

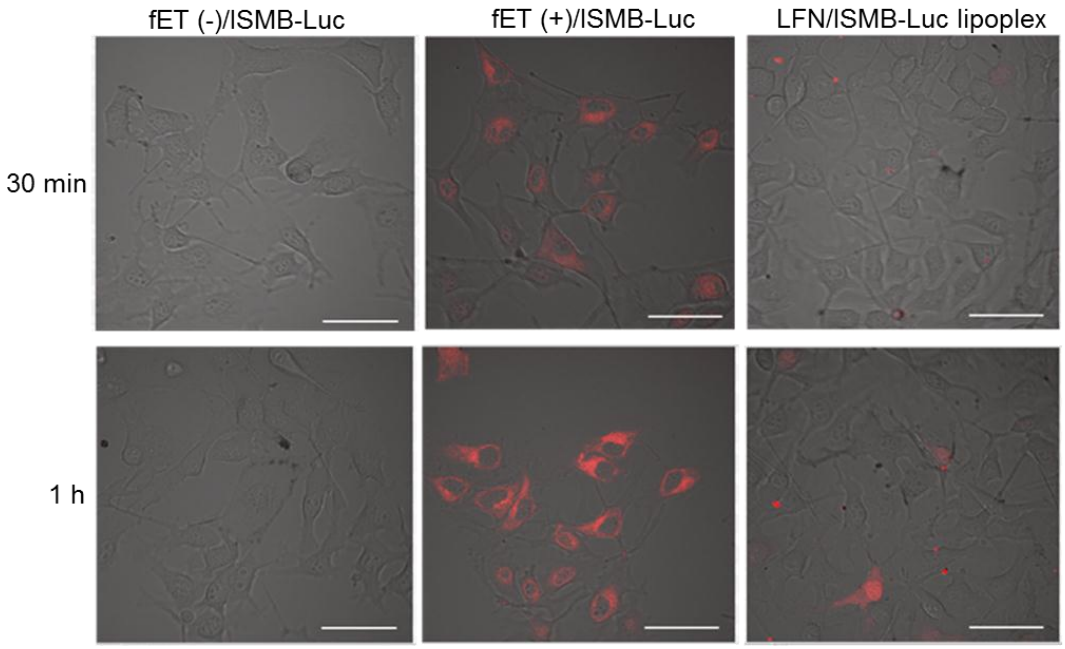

Figure 10. Cytoplasmic delivery of ISMB-Luc induced by faint fET.
Cells were treated with fET (0.34 mA/cm^2, 15 min) in the presence of ISMB-Luc solution or transfected with LFN/ISMB-Luc lipoplex. At the time points at 30 min or 1 h from the start of fET or LFN transfection, the cells were observed with a CLSM. Red fluorescence signals show cytoplasmic delivery and the association of ISMB with its targeted mRNA. Scale bars indicate 50 μm. ***J. Control. Release, 2016, 228, 20*-25, *Supplemental Figure 4.***

2-4 Determination of cytotoxicity of fET treated cells

The cytotoxicity of electricity-based delivery system such as electroporation was usually observed immediately after the treatment [40]. Thus, the cell viability immediately after fET was evaluated in this study by following trypan blue exclusion test [33]. Immediately after fET (0.34 mA/cm^2, 15 min), cells were not stained by trypan blue, thereby viability of fET-treated cells remained like non-treated cells (Figure 11). This result indicates that fET did not induce electricity based cytotoxicity such as electroporation, membrane damage, and cell death.

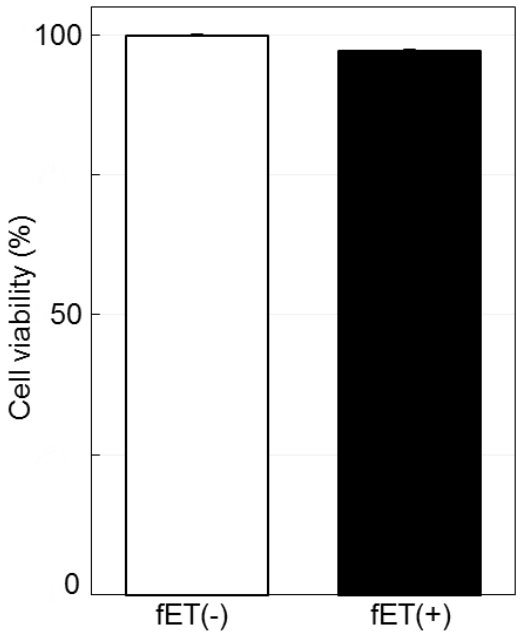

Figure 11. Cells were stained with trypan blue solution immediately after fET (0.34 mA/cm^2, 15 min). The number of stained and non-stained cells was counted. The percentage of cell viability was calculated by the formula (100 x number of non-stained cells / total number of cells). Data were obtained by three separate experiments, and are expressed as mean ± SD. **p*<0.05. ***J. Control. Release, 2016, 228,* 20-25*, Supplemental Figure 1.***

2-5 Evaluation of fET mediated cellular uptake mechanism

The effect of low temperature (0-4 ^{o}C) and endocytosis inhibitors on cellular uptake of rhodamine-labeled siRNA was assessed to investigate the intracellular delivery mechanism induced by fET. The fluorescence intensity of cellular lysate was significantly increased while fET was performed at room temperature in the presence of rhodamine-labeled siRNA, indicating that fET promoted cellular uptake of rhodamine-labeled siRNA. Low temperature exposure is usually used to non-specifically inhibit energy dependent cellular uptake pathway [41]. Thus, the effect of low temperature on fET mediated cellular uptake was examined by treating faint electricity to cells in the presence of rhodamine-labeled siRNA on ice. The significant suppression of fluorescence intensity by low temperature exposure implies that fET mediated cellular uptake of siRNA was inhibited (Figure 12). This result indicates that, fET activated biological processes involving energy dependent pathways. In the next step, the effect of clathrin-mediated endocytosis inhibitor, hypertonic sucrose, macropinocytosis inhibitor, amiloride and caveolae mediated endocytosis inhibitor, filipin on cellular uptake of rhodamine-labeled siRNA was examined to specify the cellular uptake pathway. The macropinocytosis inhibitor, amiloride and caveolae mediated endocytosis inhibitor, filipin significantly suppressed siRNA uptake while hypertonic sucrose slightly suppressed siRNA uptake (Figure 12).

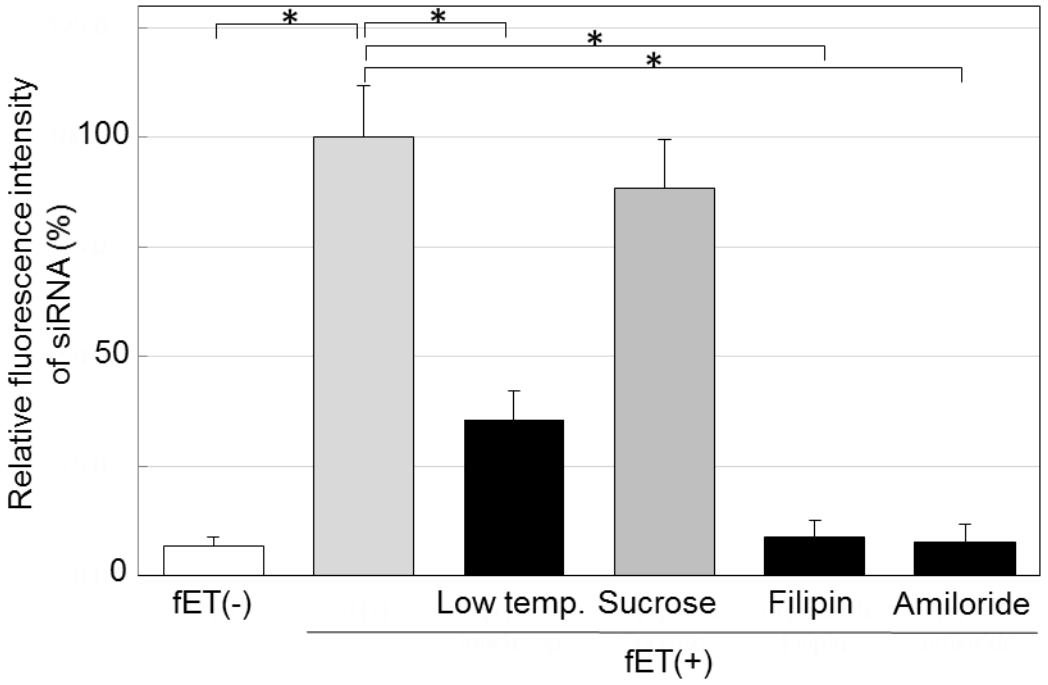

Figure 12. Assessing the effect of low temperature and endocytosis inhibitors on cellular uptake of rhodamine-labeled siRNA. fET was performed on ice for low temperature exposure. To evaluate the effect of endocytosis inhibitors, cells were pre-treated for 15 min with inhibitors prior to fET (0.34 mA/cm^2, 15 min) with rhodamine-labeled siRNA. After 1 h of fET, cells were washed and lysed and the fluorescence intensity of lysate was measured. Data were obtained by three separate experiments, and are expressed as mean ± SD. *p<0.05. ***J. Control. Release, 2016, 228, 20*-25, *Figure 2.***

2-6 Effect of fET on intracellular inflow of Ca^{2+}

Ca^{2+} influx can initiate all forms of endocytosis including slow endocytosis, rapid endocytosis, bulk endocytosis, and endocytosis overshoot during depolarization at a nerve terminal [31]. In the present section, I evaluated the effect of fET or fET with functional nucleic acid siRNA (anti-Luc) on intracellular inflow of Ca^{2+} by CLSM immediately after fET using Fluo-4 fluorescent dye. As a result, fluorescence signals equivalent to the intracellular amounts of Ca^{2+} were increased immediately after fET or fET/siRNA (Figure 13). In addition, the Fluo-4 fluorescence signals were markedly reduced while cells were pre-treated with Ca^{2+} chelator EGTA (Figure 13). This result indicates that fET-induced intracellular inflow of Ca^{2+} may activate cellular uptake of FNAs. Next, the role of Ca^{2+} influx on fET mediated cellular uptake of fluorescent-labelled siRNA was evaluated. As a result, it was found that, while cells were pre-treated with EGTA, a Ca^{2+} chelator, the cellular uptake of siRNA was significantly reduced even after fET (Figure 14). This result indicates that fET mediated intracellular influx of Ca^{2+} would change the cellular physiology such as actin cytoskeleton remodeling for cellular uptake of FNAs.

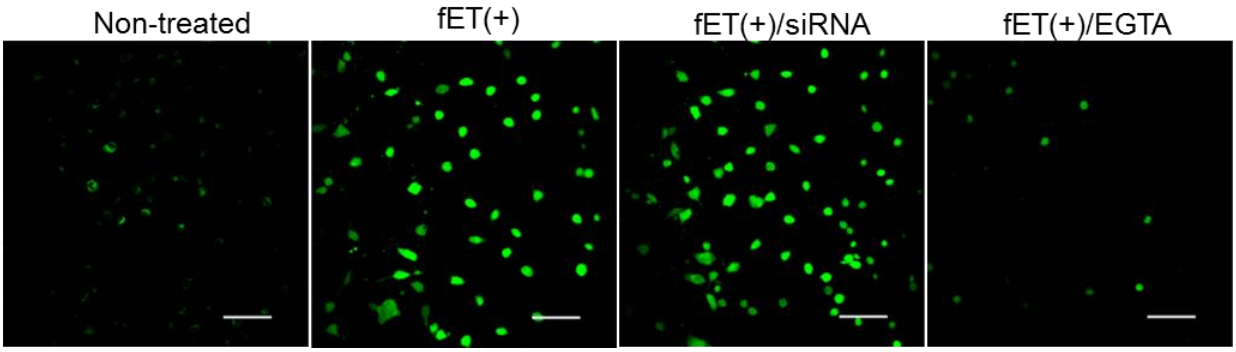

Figure 13. Effect of fET on intracellular inflow of Ca^{2+}. Ca^{2+} influx was visualized by Fluo-4 fluorescent dye and observed by CLSM immediately after fET or fET with siRNA. fET induced Ca^{2+} influx was further confirmed with pre-treatment of Ca^{2+} chelator EGTA (5mM, 30 min). Scale bars indicate 100 μm.

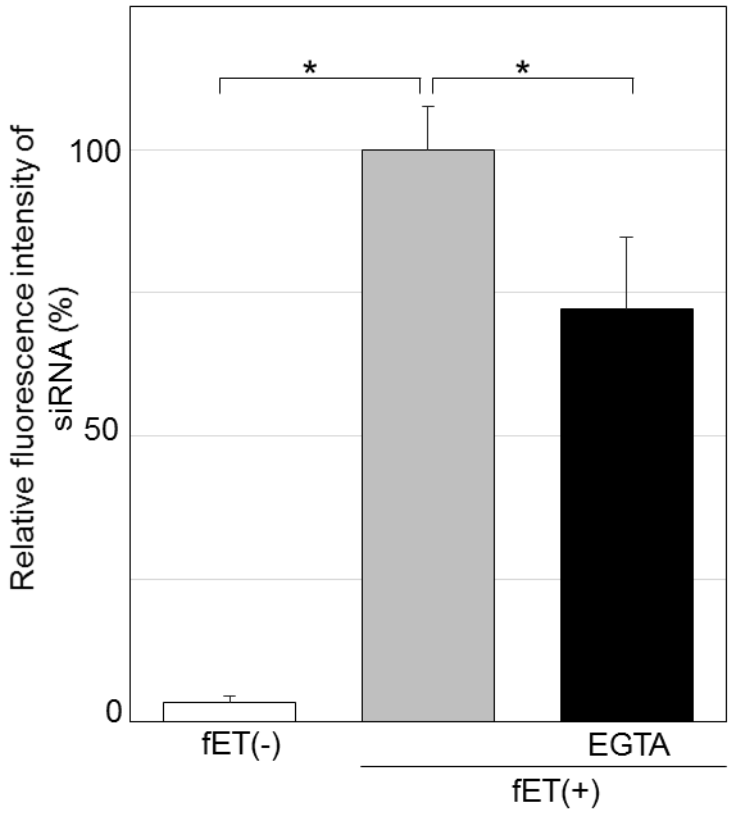

Figure 14. Effect of Ca^{2+} chelation on fET-induced cellular uptake of rhodamine-labeled siRNA. For Ca^{2+} chelation, cells were incubated with 5mM EGTA for 30 min prior to the fET (0.34 mA/cm^2, 15min) with 100 pmol rhodamine-labeled siRNA. After 1 h from the starting point of fET, cells were lysed and fluorescence intensity of the lysate was measured. Data were obtained by three separate experiments, and are expressed as mean ± SD, *p<0.05.

2-7 Effect of fET on actin cytoskeleton

The cortical actin cytoskeleton is closely associated with plasma membrane and its active remodeling is necessary for cellular uptake process. To examine the effect of fET on cytoskeletal organization, the actin cytoskeleton was stained immediately after fET with rhodamine phalloidin, followed by observation under CLSM.

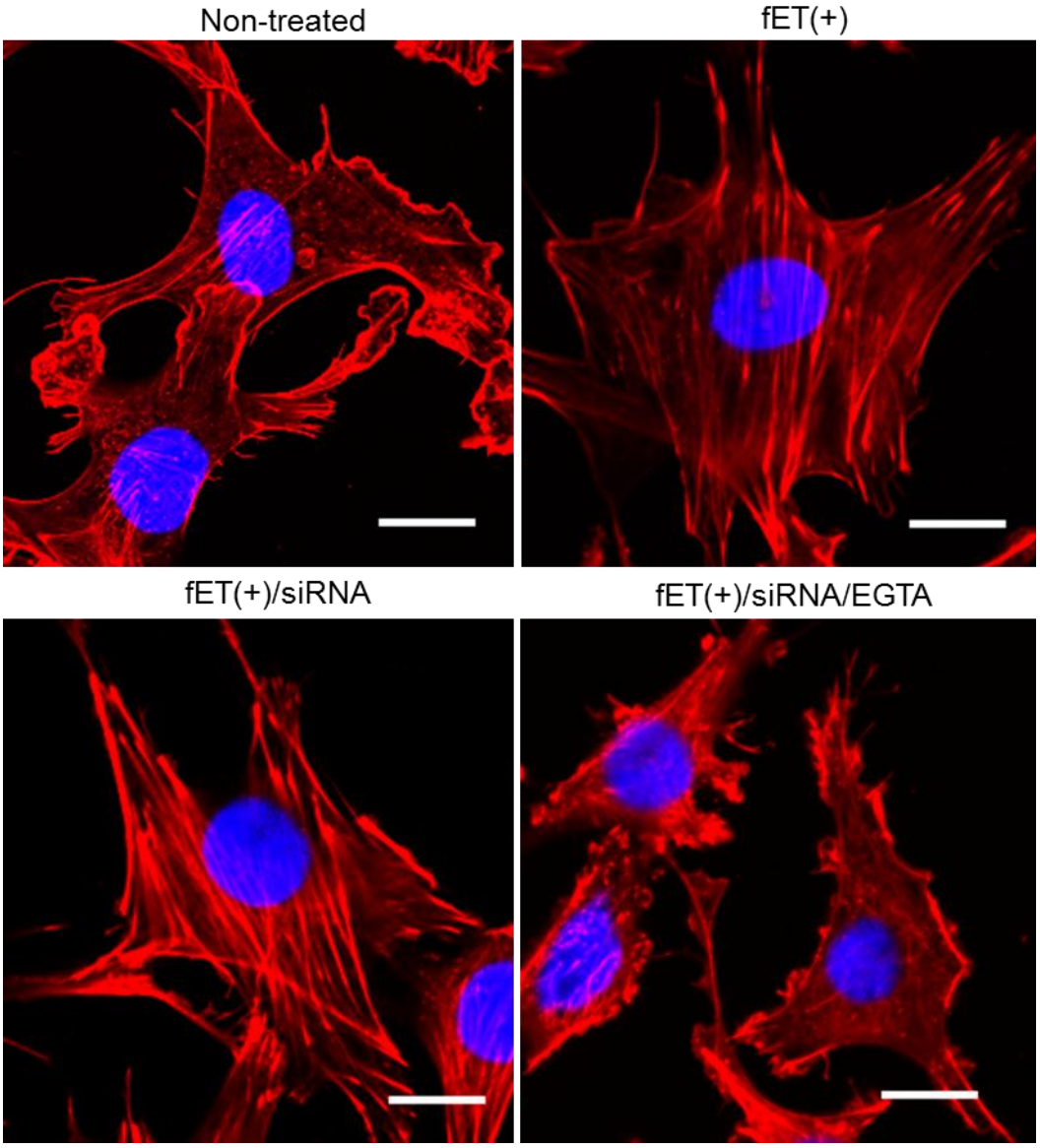

Figure 15. Evaluation of the effect of fET on actin cytoskeleton. Cells were treated with fET (0.34 mA/cm^2, 15min) or fET with siRNA, followed by actin staining. After staining, actin cytoskeletal organization was evaluated by CLSM observation. Red signals indicate rhodamine phalloidin-labeled actin while blue signals indicate nuclei. Scale bars indicate 20 μm.

Interestingly, active cytoskeleton remodeling was found after fET or fET/siRNA (anti-Luc), which is likely the outward protrusion and inward movement of cortical actin cytoskeletal network was increased. Moreover, filapodia and stress fibers formation were markedly promoted after fET (Figure 15). Furthermore, Ca^{2+} chelation by EGTA shrunk actin cytoskeleton even in cells treated with fET (Figure 15). This result indicates that fET-mediated intracellular inflow of Ca^{2+} changes cellular physiology to induce actin cytoskeletal remodeling, which may promote plasma membrane invagination and endocytic vesicle formation to activate cellular uptake process.

2-8 Evaluation of the effect of fET on membrane potential

Application of electricity to cells would affect the intracellular ion balance by activating the flow of cationic ions from outside of cell to inside the cell. The activation of cationic ion channels along with anodal electrostatic repulsion of cations may contribute to the flow of cations into cells. Thus, fET could alter the membrane potential to activate cellular uptake pathway. To check the effect of fET on membrane potential, cells were treated with fET in the presence of voltage sensitive fluorescence dye DiBAC4(3). The fluorescence intensity of cells treated with fET was found to be higher than that of control cells (Figure 16). This result indicates that fET decreased membrane potential upon inducing the influx of cations such as Ca^{2+} into cells. Intracellular amount of DiBAC4(3) was 13% increased by fET evaluated by quantitative measurement of the fluorescence intensity. In order to confirm the possibility of physical permeation of DiBAC4(3), the effect of low temperature on fET mediated cellular uptake was examined. DiBAC4(3) fluorescence intensity remained similar to control cells when fET was performed on ice, indicating that membrane potential was not changed at low temperature even after fET. Additionally, this result also indicates that fET did not physically facilitate cellular uptake of DiBAC4(3), moreover, it may activate non-specific cationic ion channels such as TRP channels to contribute the alteration of membrane potential.

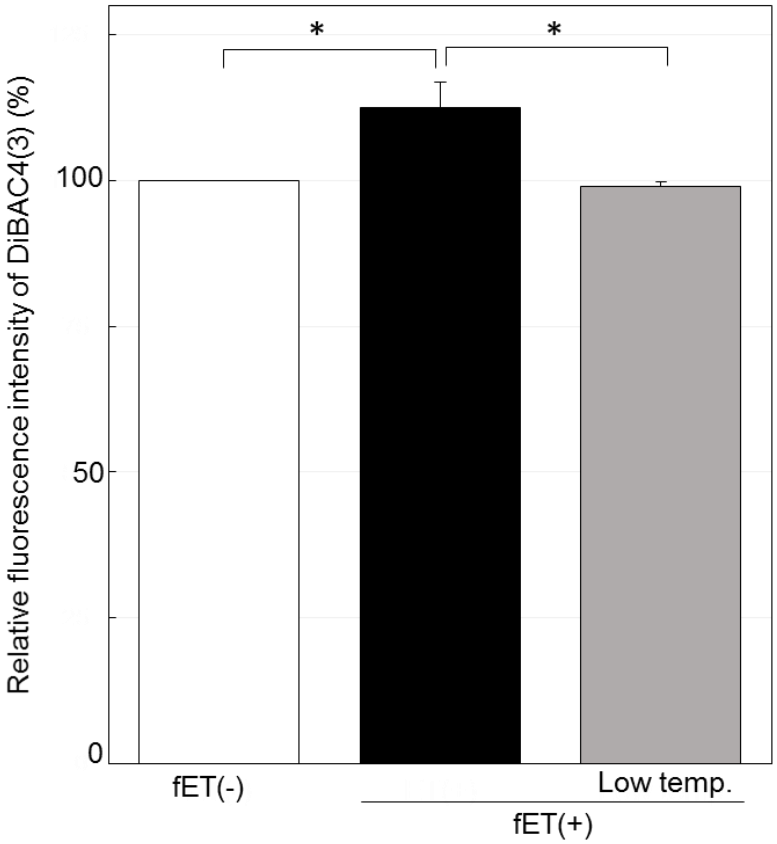

Figure 16. Evaluation of fET mediated cellular penetration of DiBAC4(3). Cells were incubated for 30 min in the presence of DiBAC4(3) followed by fET (0.34 mA/cm^2, 15 min). For low temperature exposure, fET was performed on ice. Cells were washed and lysed after fET, and fluorescence intensity of the lysate was measured. Data were obtained by three separate experiments, and are expressed as mean ± SD. *p<0.05. ***J. Control. Release, 2016, 228, 20-25, Figure 3.***

In the next step, the involvement of TRP channels in fET induced cellular uptake was evaluated by assessing the effect of the TRP channels blocker SKF96365. Cellular uptake of rhodamine-labeled siRNA by fET with SKF96365 was examined. As result, it was found that, SKF96365 significantly suppressed cellular uptake of siRNA (Figure 17). Nonetheless, this result indicates that activation of cationic channels including TRP channels may be involved at least partly in fET mediated cellular uptake process.

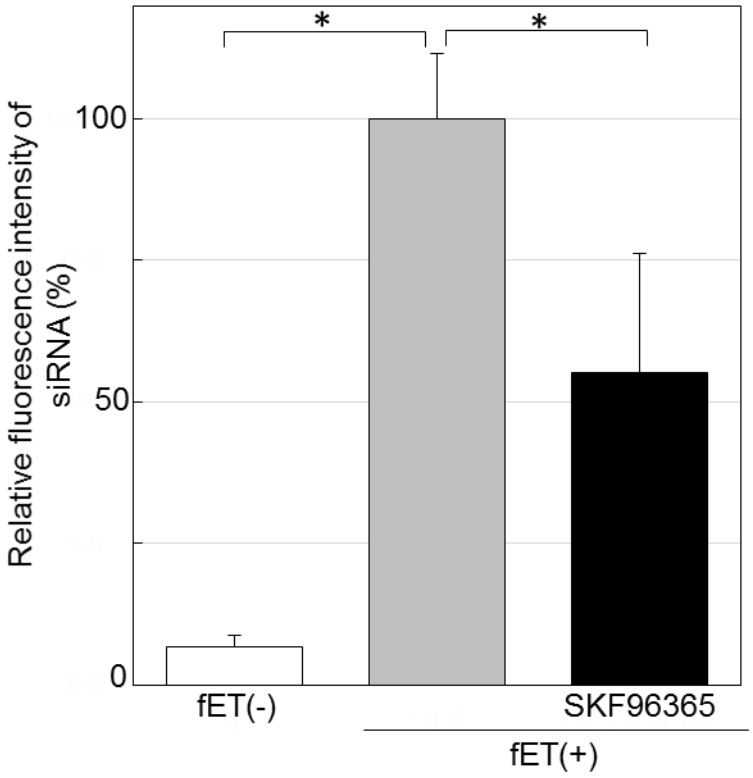

Figure 17. Effect of TRP channel inhibitor SKF96365 on cellular uptake of rhodamine-labeled siRNA. Cells were incubated 15 min with SKF96365 before being treated with fET (0.34 mA/cm^2, 15 min) in the presence of siRNA solution. After fET, cells were washed and lysed and the fluorescence intensity of the lysate was measured. Data were obtained by three separate experiments, and are expressed as mean ± SD. *p<0.05. ***J. Control. Release, 2016, 228, 20*-**25**, *Figure 4.***

3 Discussion

Intracellular delivery of functional nucleic acids is difficult to obtain because of some biological barriers present in cell including plasma membrane and endosomal membrane [42]. Thus, more advanced drug delivery technology is needed to overcome the issue of infective delivery of functional nucleic acids mediated by conventional drug delivery methods. Recently, researchers pay their attention to iontophoresis in the field of transdermal drug delivery. In addition, iontophoresis mediated *in vivo* delivery of nucleic acids into the skin is reported [26]. However, whether the faint electricity of iontophoresis induce cellular uptake or cytoplasmic delivery is remained unclear. Thus in this study, I examined the effect of *in vitro* faint electric treatment on cellular uptake and cytoplasmic delivery of functional nucleic acids. The density of electricity uses in IP ranges from 0.5 mA/cm^2 to less. Based on some previous *in vivo* studies [26, 27, 28, 29], and upon considering efficient delivery without induction of electricity based cytotoxicity, here the density of electricity was used as 0.34 mA/cm^2, 15 min.

In vitro fET of siRNA was examined and confirmed to have the significant RNAi effect. Here, the RNAi effect remained lower than positive control LFN/siRNA lipoplex. But this result suggests that, fET delivered siRNA into the cytoplasm of cells without any assistance of carriers for cellular association and endosomal escape. The higher knockdown effect of LFN/lipoplex than that of the fET/siRNA may be occurred due to the toxicity of cationic nanocarriers. It has been reported that, cationic siRNA carriers induced cellular damage by direct interaction between cationic groups and cellular components or indirectly by generating reactive oxidative species in cells [18, 43]. Thus, the nanotoxicity of LFN/siRNA would be a reason for higher RNAi effect than that of fET/siRNA.

As siRNA deliver into the cytoplasm by fET, the cytoplasmic delivery process was monitored using an oligonucleotide probe in-stem molecular beacon (ISMB). Interestingly, all cells showed potent red fluorescence after 1 h of fET with ISMB-Luc indicating that fET efficiently delivered ISMB-Luc into the cytoplasm and associated with the luciferase mRNA into the cytoplasm of cells (Figure 7). Additionally, cells showed fluorescence signals immediately after fET and the intensity of the fluorescence signals were increased with the increasing time (Figure 8), suggesting that cytoplasmic delivery was indeed enhanced by fET. Although the RNAi effect provided by fET in the presence of siRNA was weak than that of the LFN/siRNA lipoplex, the fET method delivered functional nucleic acids such as ISMB into the cytoplasm of cells very rapidly. Even in between 15 min, FNAs can be reached to the cytoplasm of cells by fET method. Moreover, from the result of comparative study of fET based delivery of ISMB and LFN based delivery of ISMB (Figures 9 & 10), it was found that while fET was performed with ISMB, then all cells in the culture dish showed fluorescence signals which means that fET induced homogeneous delivery of FNAs to all cells. On the other hand, the delivery speed of fET method was faster than that of the LFN based delivery of FNAs. Since fET deliver naked FNAs into cells, immediately after internalization and escape from endosome, FNAs can associate with their intracellular targets and show functionality. On the other hand, cationic nanostructures form complex with negatively charged FNAs via electrostatic interaction. After taken up these nanostructures by cells, it is difficult to release FNAs from the cationic carriers, leading to slow down

and reduce the transfection efficiency. Therefore, carrier independent, rapid and homogeneous delivery of FNAs are advantages of fET.

FNAs are susceptible to degradation by degradation enzymes such as nucleases either in the extracellular environment or in the endosome. In this situation, long staying of FNAs either in the extracellular environments or in the endosome reduces the functionality or degrades FNAs. Thus, rapid cellular uptake and cytoplasmic delivery by fET would reduce the exposure time of FNAs medicines to the degradation enzymes, indicating that fET would preserve the functionality of FNAs which will be useful for effective therapy. Actually, it has been reported that FNAs without any protections delivered by fET can show their functionality even though *in vivo* [26]. Additionally, fET delivers FNAs homogeneously to all target cells. Since it is reported that, as heterogeneous delivery of FNAs induced ineffective RNAi [44], siRNA is needed to deliver all cells for effective regulation of target genes. Therefore, fET-mediated homogeneous delivery will be useful for effective therapy.

From the mechanistic study, it was found that, fET increased cellular uptake of rhodamine-labeled siRNA. In Figure 11, fET-treated cells were not stained by trypan blue, suggesting that membrane damages did not contribute to effective cellular uptake and cytosolic delivery of siRNA mediated by fET. The non-specific inhibition of energy dependent pathway such as low temperature exposure significantly suppressed fET-mediated cellular uptake of rhodamine-labeled siRNA, suggesting that energy dependent pathway would be activated by fET. The macropinocytosis inhibitor amiloride, caveolae-mediated endocytosis inhibitor filipin, and clathrin-mediated endocytosis inhibitor hypertonic sucrose were used to further study the cellular uptake process. Among these inhibitors, amiloride and filipin significantly prevented fET induced cellular uptake of rhodamine-labeled siRNA, while hypertonic sucrose partially suppressed siRNA uptake, indicating that endocytosis such as macropinocytosis and caveolae-mediated endocytosis would be activated by fET. The cellular uptake of macromolecules largely depends on the surface interaction of macromolecules and cells [17]. Although it is known that clathrin-mediated endocytosis is a major uptake mechanism for nanostructures and macromolecules but fET delivers naked FNAs which negatively charged. During fET-mediated delivery of FNAs, it may be difficult for FNAs to interact with plasma membrane like cationic nanocarriers. In the contrary to the clathrin-mediated cellular uptake pathway, the present study suggests that fET may change the cortical cytoskeletal remodeling to induce actin-based cell surface ruffling to activate cathrin independent cellular uptake pathways (Figures 14 & 15). Here, the inhibitory effects of amiloride and filipin are more potent than that of low-temperature exposure, although low-temperature exposure can inhibit all cellular uptake pathways. Amiloride usually inhibits Na^+/H^+ exchange and also affects actin cytoskeleton while filipin binds with the cholesterol on plasma membrane. In the present study, inhibitory experiments were performed at the condition without cytotoxicity of inhibitors according to the previous reports [34, 35, 36]. The role of Na^+/H^+ exchange has been well studied in cardiomyocytes and reported that the inhibition of Na^+/H^+ exchange can prevent Ca^{2+} overload and reduce intracellular concentration of Ca^{2+} [45]. On the other hand, it has been also reported that the reduced cholesterol level at plasma membrane limits Ca^{2+} influx into cells [46]. Thus, the membrane potential may not change in the cells treated with amiloride or filipin even after fET, leading to more potent inhibition of the cellular uptake

of siRNA in comparison with low temperature treatment. Although it may be difficult to specify which type of cellular uptake process is activated by fET, macropinocytosis and caveolae-mediated endocytosis may be the possible cellular uptake pathway activated by fET.

Furthermore, the cellular penetration of DiBAC4(3) was increased by fET, indicating that membrane potential of cell was altered by fET. The fluorescence response of the voltage sensitive dye DiBAC4(3) was reported to be about 1% per 1 mV [47]. Herein, fET induced the increase in fluorescence of DiBAC4(3) by 13% than that of control cells. This result means that fET decreases the membrane potential approximately 13 mV to depolarize cells. Additionally, fluorescence intensity of DiBAC4(3) did not increase at low temperature even after fET, suggesting that membrane potential was changed via biological mechanism such as activation of cationic ion channels, not physical factor such as membrane disruption. Moreover, the activation of non-specific cationic channels such as TRP channels [48] was found to be involved in the fET mediated cellular uptake, because TRP channel blocker suppressed cellular uptake of siRNA induced by fET. Together, these results suggest that membrane potential changes via activation of cationic channels, such as TRP channels, play a role in contributing to fET activated cellular uptake of FNAs. TRP channels are recognized as cellular sensors. They can sense temperature, pain, taste, osmolality, and other stimuli to adapt cells with extracellular environment. However, the gating mechanism of TRP channels remains still poorly understood. Several hypothesizes such as cell sensory hypothesis, receptor operated theory, or store-operated calcium entry hypothesis describe the activation of TRP channels [49]. Based on the cell sensory hypothesis, the result of Figure 17 suggests that, during fET, TRP channels may sense electromotive force or any other factors such as fET induced electro-osmosis, electrostatic repulsion, or temperature fluctuation may be responsible for the activation of TRP channels. Therefore, fET appears to regulate physiology of cells by depolarizing membrane upon promoting cationic ions influx. The magnitude of the membrane potential in many cells is approximately -70 mV and it has been reported that, the changes of the membrane potential toward the depolarization soften the plasma membrane [50]. In addition, it has also been reported that plasma membrane depolarization activates Rho small GTPase family protein which is a major regulator of actin cytoskeleton and associated with cellular uptake process [51, 52]. Thus, the co-operative effect of depolarized membrane such as changes the stiffness of the plasma may facilitate membrane ruffling while activation of signaling molecules induces actin cytoskeleton remodeling, contributing to the cellular uptake process.

In this chapter, fET induced rapid and homogeneous delivery of FNAs into cells by activating biological processes without any assistance of carriers. fET mediated alteration of membrane potential via the activation of cationic ion channels leads to the cellular uptake process endocytosis. Thus, fET would be a safe and efficient intracellular delivery technology of FNAs for the effective regulation of target genes.

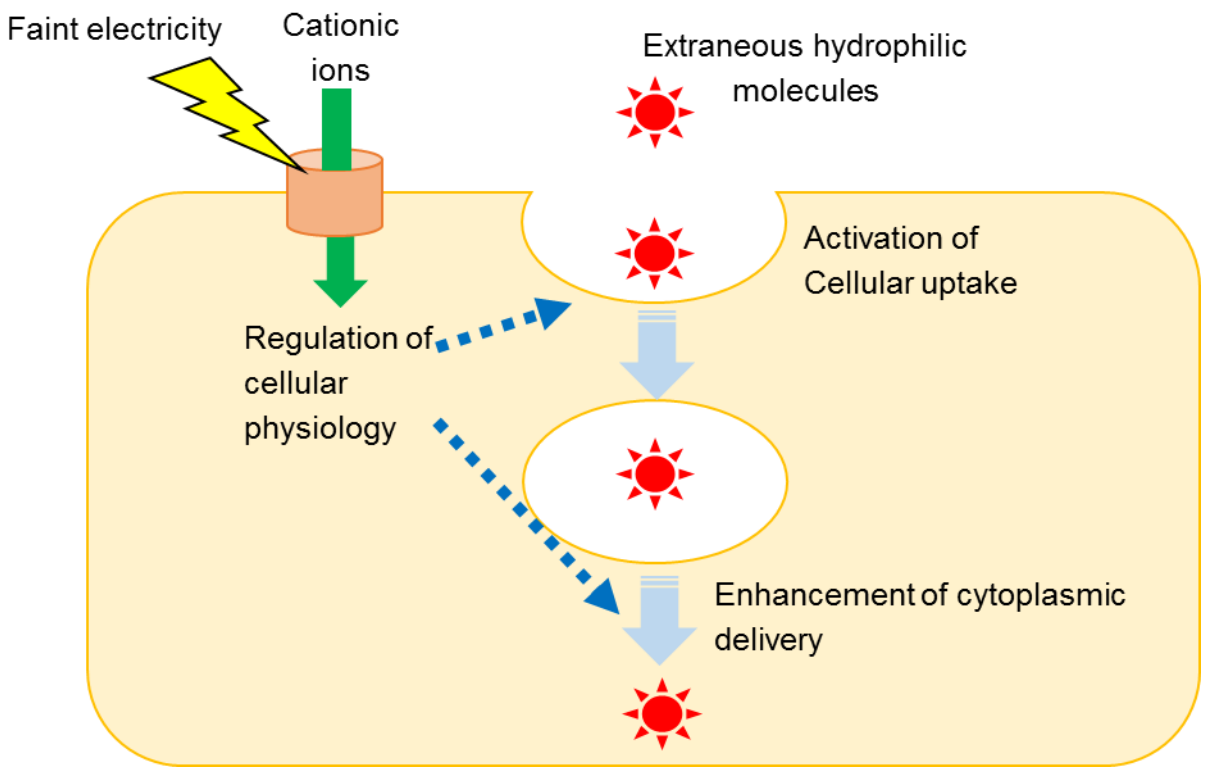

Figure 18. Graphical summary of chapter I. Application of faint electricity activates cationic ion channel on plasma membrane to induce the influx of cations such as Ca^{2+} into cell. Influx of cations changes membrane potential and may activate downstream signaling molecules to change cellular physiology leading to the cellular uptake process. ***J. Control. Release, 2016, 228, 20-25, Graphical abstract.***

Chapter II. The novel functional nucleic acid iRed effectively regulates target genes following cytoplasmic delivery by faint electric treatment

In the first chapter, I evaluated that fET activated rapid and homogeneous delivery of FNAs into the cells by activating cellular uptake process. In this chapter, the intracellular delivery of a novel functional nucleic acid intelligent shRNA expression device (iRed) is examined by fET.

RNAi is the fundamental mechanism to regulate the target gene expression in cells. Usually, chemically synthesized siRNA and plasmid expressing shRNA are used to induce RNAi effect in cells. However, each tool has some difficulties to use [53, 5]. Such as, the stability of siRNA is lower than that of the DNA. In contrary, the molecular size of plasmid DNA is huge, and CpG motif present in the shRNA-encoding plasmid induces innate immune response [54]. Thus, to improve the drawbacks of RNAi effect providing tools, iRed is developed [55]. iRed consists of 4'-thiol DNA amplified by polymerase chain reaction (PCR) . It encodes a minimum essential sequence of shRNA in cells such as U6 promoter and shRNA encoding region in which any one type of adenine (A), guanine (G), cytosine (C), or thymine (T) nucleotide unit was substituted by each cognate 4'-thio derivatives, i.e., dSA iRed, dSG iRed, dSC iRed, and ST iRed, respectively. Depending on the substituted nucleotides, several types of iRed have been existed. Among them, cytosine nucleotide substituted by 2'-Deoxy-4'-thiocytidine 5'-Triphosphate (dSCTP) based iRed, such as dSC iRed is reported to be superior regarding their potent RNAi effect into cells [55]. Therefore, dSC iRed is used in this study. As a thiol DNA, dSC iRed shows resistance against nuclease degradation. Thus, the stability of dSC iRed is higher than siRNA in physiological environment. On the other hand, the molecular size of dSC iRed is also lower compared to conventional plasmid DNA. Additionally, even one copy of dSC iRed enter into the nucleus then it can produce numerous copy of shRNA in cells [55].

To effectively regulate target genes by iRed, the development of rational delivery method for iRed is needed. Non-viral vectors composing of cationic polymers or lipids are mostly expected as the delivery method for RNAi devices, and are constructed by using the electrostatic interaction of cationic materials with nucleic acids. It has been reported that cationic materials can also bind to endogenous mRNA in the cytoplasm of cells via electrostatic interaction, resulting in the non-specific regulation of mRNA as well as undesirable cytotoxicity derived from cationic materials [56, 57, 58]. When cationic materials-based non-viral vectors are used for the intracellular delivery of iRed, they impede the functions of dSC iRed via the undesirable electrostatic interaction of cationic materials with newly synthesized shRNA from dSC iRed in the transfected cells. Thus, a new delivery technology besides carrier-based delivery system is desirable for intracellular delivery of dSC iRed.

As described in chapter I, fET can achieve the effective intracellular delivery of FNAs without any assistance of carriers such as cationic polymers or lipids. Therefore, I examined the effect of fET on intracellular delivery of this novel functional nucleic acids dSC iRed. In this study, to monitor the intracellular delivery of dSC iRed against luciferase by fET, B16F1 cells stably expressing luciferase were

used. Moreover, to obtain the functional evidence of dSC iRed delivered by fET, I examined the effect of dSC iRed against resistin as a key molecule in obesity on lipid accumulation of 3T3-L1 adipocytes model.

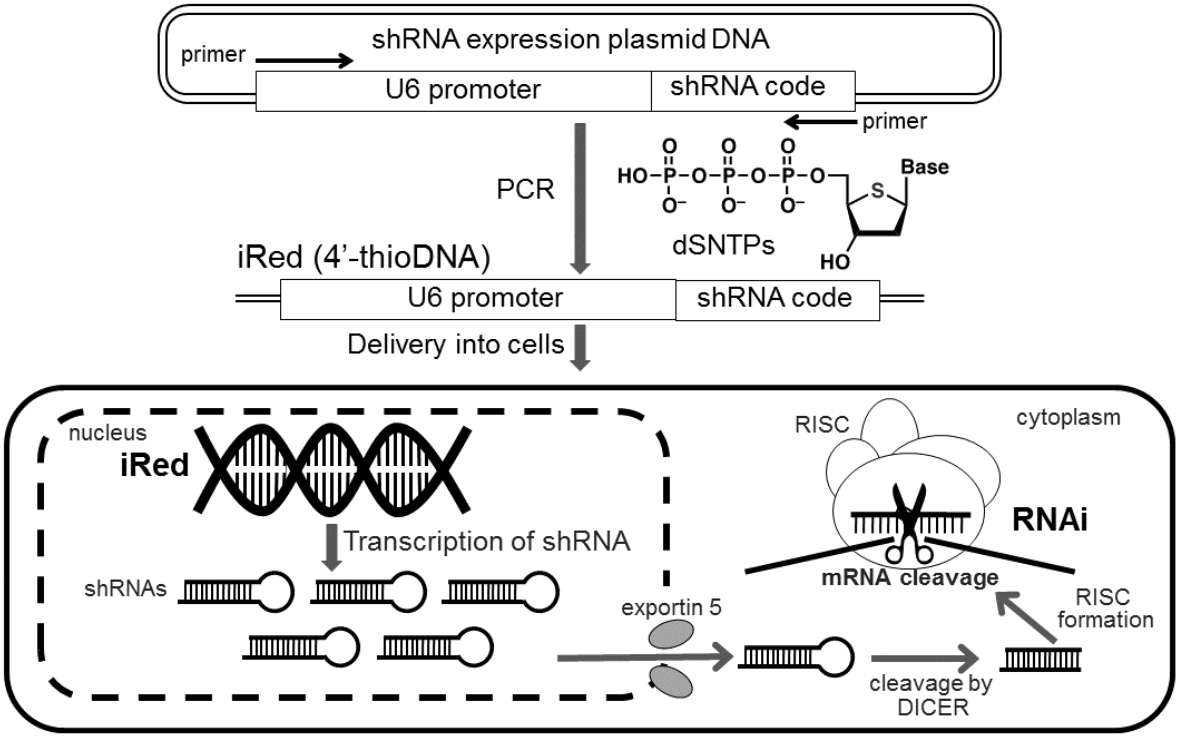

Figure 19. Schematic image of dSC iRed preparation and transcription of shRNA for RNAi effect. Step 1. Preparation of dSc iRed by PCR amplification of region encoding U6 promoter and shRNA in the presence of dSNTP. Step 2. Delivery of dSC iRed into the nucleus of the target cells. Step 3. shRNAs are produced in the nucleus from the iRed. Then, shRNAs are exported from the nucleus and RNAi is evident. ***Sci. Technol. Avd. Mater. 2016, 17, 554-562, Figure 1.***

1 Materials and methods

1-1 Cell culture

The mouse melanoma cell line B16F1 was purchased from Dainippon Sumitomo Pharma Biomedical Co., Ltd. (Osaka Japan). The clone of B16F1 cells expressing luciferase (B16F1-Luc) was established in our laboratory [39]. These cells were cultivated in Dulbecco's modified Eagle's medium (DMEM) supplemented with 10% fetal bovine serum (FBS) at 37 ^{o} C in 5% CO_2. The 3T3-L1 cell line was obtained from the Japan Health Sciences Foundation (Tokyo, Japan). The culture and induction of differentiation of 3T3-L1 cells were performed according to the procedures described below.

1-2 Materials

Natural dNTPs were purchased from GE Healthcare Japan (Tokyo, Japan). 2'-Deoxy-4'-thionucleoside triphosphates (dSNTPs) were prepared at the laboratory of Bioorganic Chemistry, Tokushima University, Japan [59]. Oligonucleotides were purchased from FASMAC (Kanagawa, Japan). Rhodamine-labeled anti-GFP siRNA (21-mer, 5'-GCUGACCCUGAAGUUCAUCTT-3', 5'-GAUGAACUUCAGGGUCAGCTT-3') was synthesized from Invitrogen Life Technologies (Carlsbad, CA, U.S.A). Dextran labeled with fluorescein isothiocyanate (FITC), of which molecular weights were 10,000 and 70,000 was purchased from Tokyo Kasei (Tokyo, Japan). BCA protein assay kit and LysoTracker Red DND-99 were obtained from Thermo Fisher Scientific Inc (Waltham, MA). Chloroquine, D-biotin and ascorbate were purchased from Nacalai tesque (Kyoto, Japan). Lipofectamine 2000 (LFN) was purchased from Invitrogen Life Technologies (Carlsbad, CA, U.S.A). Luciferase assay substrate and cell lysis buffer were purchased from Promega Corporation (Madison WI, USA). 3,3',5-Triiodo-L-thyronine (T3), L-thyroxine (T4), 3-isobutyl-1-methylxanthine, dexamethasone, insulin, Oil Red O and Hoechst33342 were purchased from Sigma Aldrich (St. Louis, MO, USA). Formalin solution was obtained from Wako Pure Chemical Industries (Osaka, Japan)

1-3 Synthesis of dSC iRed

dSC iRed was synthesized at the laboratory of Bioorganic Chemistry, Tokushima University, Japan [55]. The procedures are as follows: for construction of shRNA expression plasmid DNA, oligonucleotides encoding sequences of shRNA and terminator were ligated to a site digested with BamHI and EcoRI of a shRNA expression cassette containing U6 promoter (RNAi-Ready pSIREN-RetroQ, Clontech, Mountain View, CA) according to the manufacturer's instructions. The inside sequences are luciferase and resistin such as for luciferase (5'-AATTCAAAAAACTTACGCTGAGTACTTCGACAACCAGGAGCACTATCGAAGT ACTCAGCGTAAG-3') and for resistin (5'-AATTCAAAAAAGCGCTGCTGGTGCCAACCCTCTCTTG AAGGGTTGGCACCAGCAGCGCG-3'), respectively. Then, to prepare iRed, PCR was performed using the shRNA expression plasmid DNA as a template. The sequences of U6 promoter and shRNA in plasmid DNA were amplified in 20 μl KOD buffer containing KOD Dash DNA polymerase (0.05 unit/μl, TOYOBO, Osaka, Japan), template plasmid DNA (0.1 fmol/μl), 200 μmol/l dNTPs, and 0.5μmol/l primers. Then, PCR was performed as follows: initial denaturation at 94 °C for 15 s, 15 cycles of denaturation/amplification (94 °C, 30 s; 62 °C, 30 s; 72 °C, 30 s), and final extension at 72 °C for 15 min. Amplicons were subjected to 1% agarose gel electrophoresis, and the DNAs were purified with a High Pure PCR Product Purification Kit (Roche, Basel, Swizerland). After purification, the second PCR amplification using the purified DNA as a templates was performed. The 100 μl reaction mixture consisted of KOD Dash DNA polymerase (0.1 unit/μl), a template DNA (0.2 fmol/μl), 200μmol/l nucleoside 5'-triphosphate mixture containing one type of dSTNP and three types of dNTPs, and 1.25 μmol/l of primers. The second PCR performed as follows: initial denaturation at 94 °C for 15 s, 30 cycles of denaturation/amplification (94 °C, 30 s; 62 °C, 30 s; 72 °C, 10 min), and final extension at 72 °C for 15 min. The iRed amplicons were purified with a High Pure

PCR Product Purification Kit (Roche). FITC-labeled dSC iRed was prepared following same protocol but with 5'-FITC labeled 5'-primer.

1-4 fET of cells

fET was performed as described in chapter I. For *in vitro* fET, cells were seeded on 35 mm dishes. The number of cells used is mentioned in each section below. After 18 h of cultivation, cells were washed with PBS, and then 800 μl serum free DMEM containing 100 pmol iRed, or 100 pmol fluorescent-labeled siRNA with or without 100 μM chloroquine was added to the cells. Ag-AgCl electrodes with 2.5 cm^2 surface area (3M Health Care, Minneapolis, MN, USA) were placed into the dish, and cells were treated with a constant current of 0.34 mA/cm^2 for 15 min.

1-5 Transfection of dSC iRed and measurement of luciferase activity

B16F1-Luc cells at a density of $1x10^4$ cells were seeded on 35 mm culture dishes. After 18 h of seeding, cells were washed with PBS, followed by addition of 1 ml serum free DMEM containing 100 pmol dSC iRed encoding anti-luciferase shRNA with or without 100 μM chloroquine. Then, fET was performed as described above. After 3 h of fET, 1 ml DMEM containing 10% FBS was added to the dishes and incubated for 21 h. After the incubation, cells were lysed by reporter lysis buffer (Promega) according to the manufacturer's protocols. The luciferase assay substrate was added to the lysate and chemiluminescence intensity was measured by a luminometer (Lumnescensor-PSN, ATTO Corp., Tokyo, Japan). The total protein concentration was assessed with BCA protein assay kit according to the manufacturer's protocols.

1-6 Measurement of fluorescent labeled siRNA uptake after fET

To measure the amount of cellular uptake of siRNA, B16F1-Luc cells at a density of $1x10^4$ cells were seeded on 35 mm culture dishes. After 18 h of cultivation, cells were washed with PBS followed by addition of 1 ml serum free DMED containing 100 pmol rhodamine-labeled siRNA to the dishes. Then, fET was performed as described above. After fET, cells were incubated for 3 h at 37 ^oC. After incubation, cells were washed with PBS and lysed with reporter lysis buffer according to the manufacturer's protocols. The fluorescence intensity of the lysate was then measured by a microplate reader (Tecan Group Ltd., Mannedorf, Switzerland) at the excitation and emission wavelengths of 546 nm and 590 nm, respectively.

1-7 Confocal laser scanning microscopy of cells after fET

$5x10^4$ B16F1-Luc cells were seeded on 0.002% poly-L-Lysine coated 35 mm glass bottom dishes for evaluation of intracellular delivery of FITC-dextran 10,000 or FITC dextran 70,000. After 18 h of cultivation, cells were washed with PBS, followed by fET (0.34 mA/cm^2 for 15 min) in the presence of 5 μM FITC-dextran 10,000 or 0.5 μM FITC-dextran 70,000. After fET, the cells were incubated for 30 min at 37 °C in 5% CO_2. Then, 0.1 μL of lyso tracker red DND-99 was added into the culture medium, and the cells were incubated for 30 min at 37 °C. After incubation, the cells were observed with a confocal laser scanning microscope LSM 700 (Carl Zeiss, Germany).

1-8 Culture and induction of differentiation of 3T3-L1 cells, and transfection of dSC iRed resistin

3T3-L1 pre-adipocytes were cultured, and differentiation into adipocytes was induced according to the previous report [60]. The procedure is as follows: cells were cultured in the basal medium (DMEM supplemented with 10% FBS, 10 mM HEPES, 0.2% $NaHCO_3$, 4 mM L-glutamine, 3.5 % (w/v) glucose, 0.2 mM ascorbate, 1 mM T3 and 30 M T4) at 37 °C under a humidified atmosphere containing 5 % CO_2. The day when cells reached confluence was defined as day 0. Adipocyte differentiation was induced by incubation in the differentiation medium (basal medium containing 500 μM 3-isobutyl-1-methylxanthine, 1 mM dexamethasone and 1.6 μM insulin) from days 0 to 2, followed by induction of maturation in the maturation medium (basal medium containing 1.6 μM insulin and 15 μM D-biotin). The cells at day 2 were treated with electricity in the presence of dSC iRed encoding anti-resistin shRNA as described above. The accumulation of lipid droplets was evaluated at day 4.

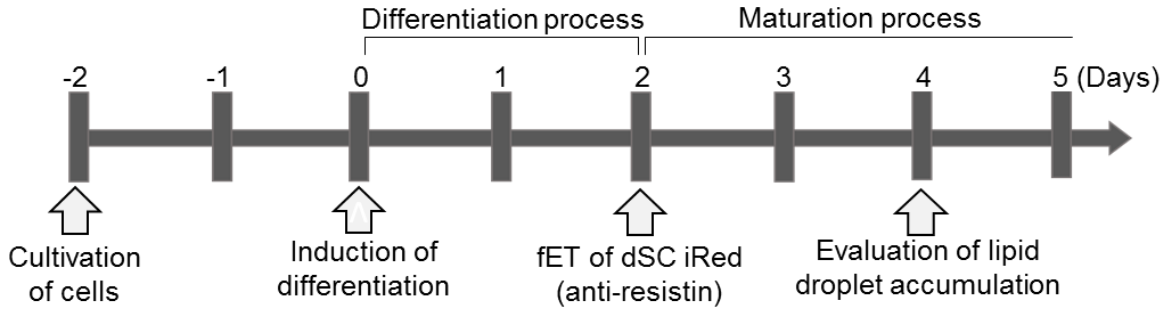

Figure 20. Time schedules of cultivation, induction of differentiation, and maturation of 3T3-L1 cells.

1-9 Measurement of lipid droplets in adipocytes by Oil Red O staining

At day 4, which means 2 days after fET and addition of the maturation medium, 3T3-L1 cells were washed with PBS and fixed with 10% (v/v) formaldehyde solution. After fixation, cells were washed with PBS and then fixed cells were incubated with 18 mg/ml Oil red O in a 60% (v/v) 2-propanol solution for 20 min at room temperature in dark. After the incubation, cells were washed with PBS and observed under microscopy. After observation, the Oil Red O dissolved in the lipid droplets was extracted by 100% 2-propanol, and its relative concentration was determined with measuring the absorbance at 540 nm by microplate reader (Tecan Group Ltd., Mannedorf, Switzerland).

1-10 Evaluation of the intracellular trafficking of dSC iRed in 3T3-L1 cells

3T3-L1 cells at a density of $5x10^4$ cells were seeded on 0.002% poly-L-Lysine coated glass bottom dish for evaluation of intracellular fate of dSC iRed after fET mediated transfection. After 18 h of cultivation, cells were washed with PBS and 1 ml of serum free medium containing 100 pmol FITC dSC iRed with or without 100 μM chloroquine was added to the dishes, followed by fET as described above. After fET, cells were incubated at 37 ºC for 2.5 h with 5% CO_2. Lyso tracker Red DND-99 at the final concentration 250 nM was added to the dish to stain endosomes or lysosome, followed by incubation for another 30 min. After incubation, 10 μl (2.5 mM) Hoechst 33342 was added to the dish to stain nucleus. After washing with PBS, cells were observed with CLSM A1R+ (Nikon Co. Ltd. Tokyo, Japan).

1-11 Statistical analysis

Statistical analysis was determined using one-way ANOVA followed by Turkey-Kramer HSD test. *p* values <0.05 were considered to be significant. They were evaluated using by JMP software (SAS Institute Inc., Cary, NC, USA)

2 Results

2-1 Transfection of dSC iRed by fET

At first, transfection of dSC iRed encoding anti-luciferase shRNA by fET on B16F1-Luc cells stably expressing luciferase was performed, and compared with transfection of dSC iRed/LFN lipoplexes. As a result, dSC iRed/LFN lipoplexes significantly reduced luciferase activity (Figure 21), indicating that shRNA produced from dSC iRed in the cells has functionality as RNAi device as reported previously, although the knock down effect was not so potent. On the contrary to the expectation, iRed/fET showed no significant effect on luciferase activity.

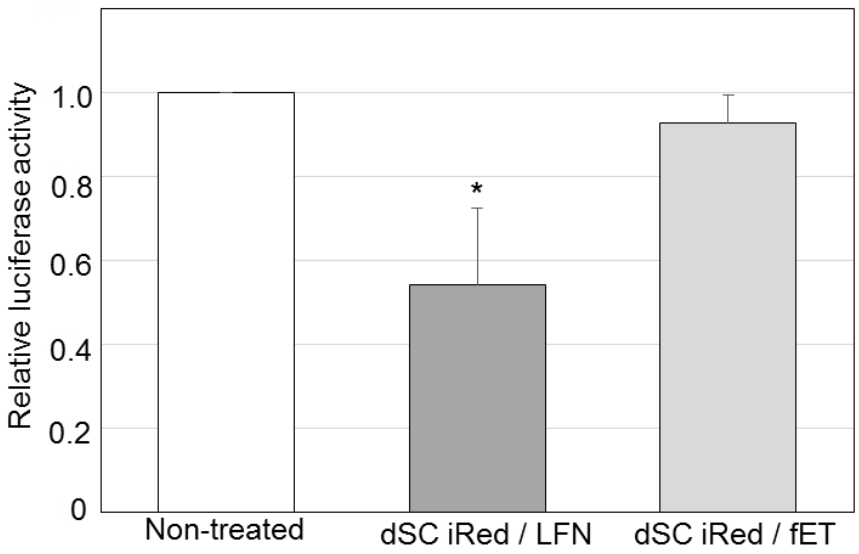

Figure 21. Transfection of dSC iRed encoding anti-luciferase shRNA in B16F1-Luc cells. Luciferase activity of B16F1-Luc cells was measured after 24 h of fET (0.34 mA/cm^2, 15 min) in the presence of dSC iRed solution. LFN/dSC iRed lipoplex was used as a positive control. Data were obtained from three separate experiments and expressed as mean ± SD. *p<0.05. ***Sci. Technol. Avd. Mater. 2016, 17, 554-562, Figure 2.***

2-2 Cellular uptake of functional nucleic acids (FNAs) by fET

To clarify the reason why dSC iRed/fET did not show significant RNAi effect, the cellular uptake of functional nucleic acids siRNA by fET was examined. In this experiment, rhodamine-labeled anti-GFP siRNA was used instead of dSC iRed. Fluorescent intensity of the cells treated with LFN/siRNA lipoplexes increased, indicating that siRNA was taken up by cells. Surprisingly, the fluorescence intensity of cells treated by electricity was significantly higher (3-fold) than that by the lipoplexes (Figure 22). This result indicates that cellular uptake by fET is more rapid than cationic nanoparticles. Before this experiment, we predicted that the uptake amount of siRNA by fET would be lower than that by LFN lipoplex because

condensed cationic nanoparticles/siRNA lipoplexes would be more effectively bound on cell surface than uptake of siRNA solution. Thus, more incubation time would be needed for cationic nanoparticles/siRNA lipoplexes to deliver cargo into cells than fET based method.

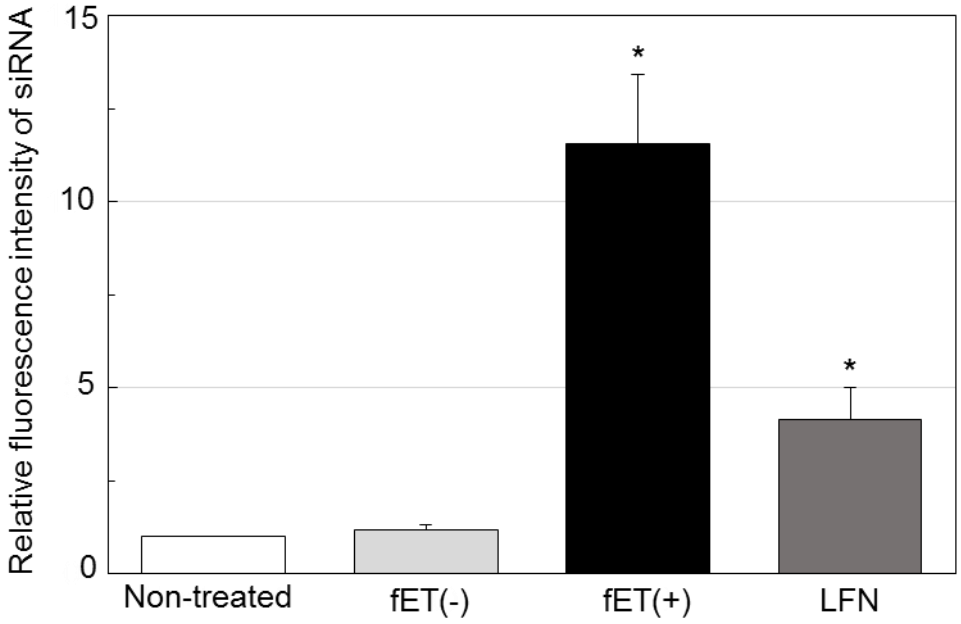

Figure 22. Relative fluorescence intensity of cells after fET in the presence of rhodamine-labeled siRNA. fET (0.34 mA/cm^2, 15 min) of cells was performed in the presence of rhodamine-labeled siRNA. After 3 h of fET, cells were washed with PBS and lysed, the fluorescent intensity of lysate was measured. . Data were obtained from three separate experiments and expressed as mean ± SD. *p<0.05. ***Sci. Technol. Avd. Mater. 2016, 17, 554-562, Figure 3.***

2-3 Evaluation of the effect of molecular size of materials on intracellular trafficking after fET

From the results of Figures 22 and 9, I found that fET induced efficient delivery of functional nucleic acids such as siRNA and ISMB into cell cytoplasm. Low functionality of iRed delivered by fET may be due to the inferior endosomal escape and nuclear delivery of dSC iRed, not the cellular uptake. It has been reported that the molecular size of macromolecules affects their intracellular trafficking. The molecular weight of iRed (MW: 225,000) is much larger than that of siRNA (MW: 11,200). Next, cells after 24 h of fET in the presence of dextran labeled with fluorescein isothiocyanate (FITC) having molecular weights 10,000 and 70,000 were observed by CLSM. As a result, potent green fluorescence signals were widely observed regarding FITC-dextran 10,000 after 24 h of fET, although fluorescence signals of endosome/lysosome were very weak (Figure 23). But, in cells without fET, red signals of endosomes were observed (Figure 24). This result indicates that FITC-dextran 10,000 was released from endosome after fET. On the other hand, dots-like green fluorescence signals were observed in the cell regarding FITC-dextran 70,000 (Figure 23), suggesting that FITC-dextran 70,000 may still remain in the endosome even after 24 h

of fET. Therefore, these results indicate that the endosomal escape efficiency of materials taken up by fET was dependent on their molecular weights.

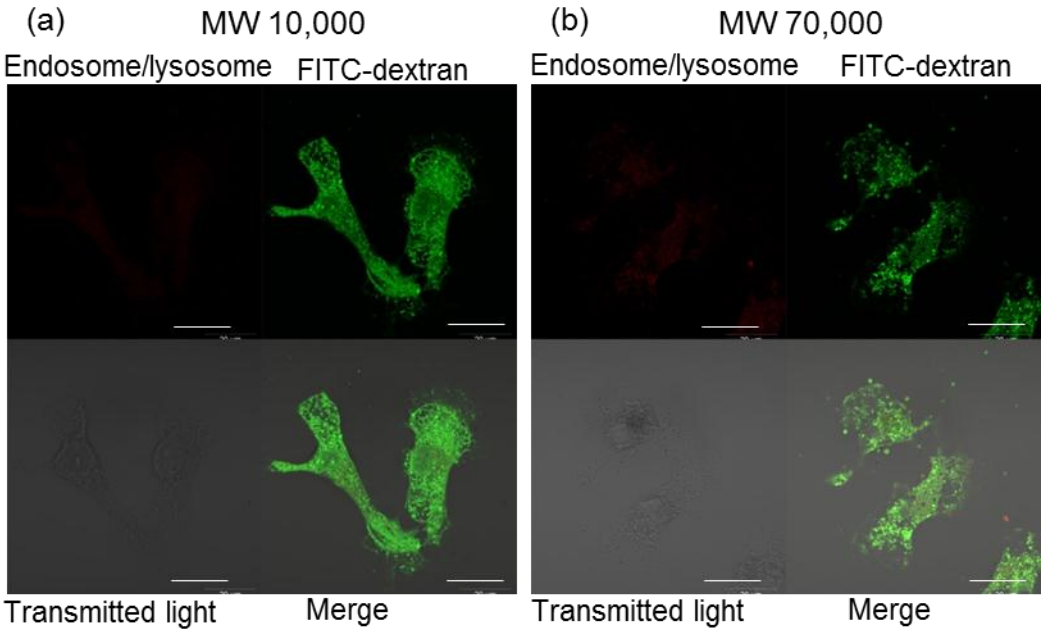

Figure 23. Confocal microscopy of cells after 24 h of fET in the presence of (a) FITC-dextran10,000 (b) FITC-dextran70,000. Cells were stained with lyso tracker red for 30 min after 23.5 h of fET with dextran solution following observation by CLSM. Scale bars indicate 20 μm. ***Sci. Technol. Avd. Mater. 2016, 17, 554-562, Figure 4.***

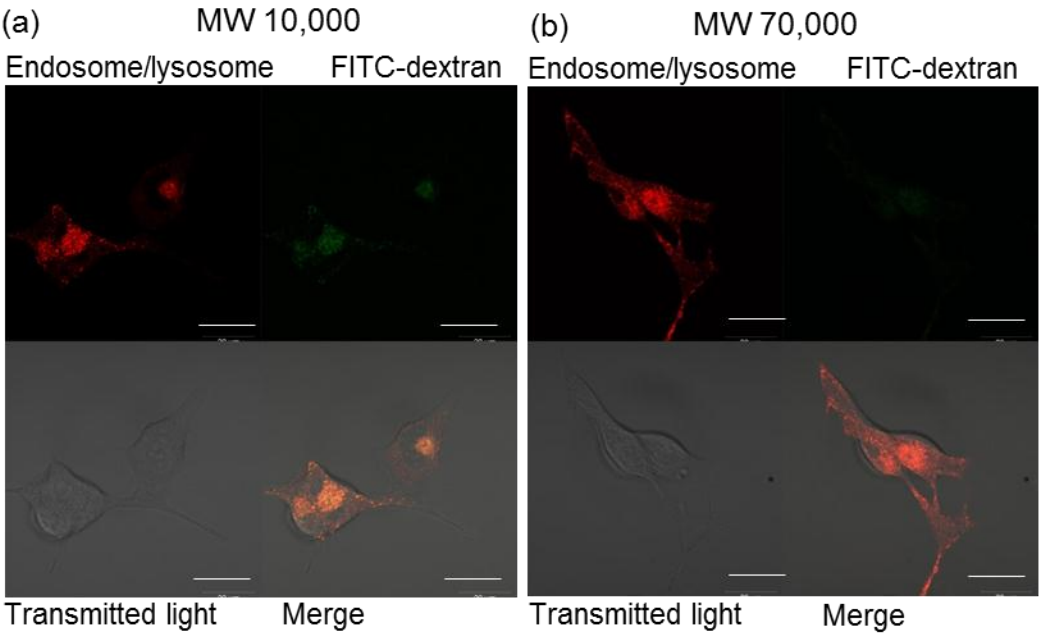

Figure 24. Confocal microscopy of cells after 24 h without fET in the presence of (a) FITC-dextran10,000, (b) FITC-dextran70,000. Cells were stained with lyso tracker red for 30 min after 23.5 h, followed observation by CLSM. Scale bars indicate 20 μm. ***Sci. Technol. Avd. Mater. 2016, 17, 554-562, Supplemental Figure 1.***

2-4 Enhancement of fET-mediated transfection of dSC iRed by improving endosomal escape

Chloroquine is known as a lysosomotropic agent. It can accumulate in endosomes or lysosomes to increase endosomal escape and enhance cytoplasmic delivery of extraneous materials [61, 62]. Thus, to improve endosomal escape of iRed internalized by endocytosis, fET with dSC iRed was performed in the presence of chloroquine. As a result, it was found that the luciferase expression was significantly suppressed by fET of dSC iRed in the presence of chloroquine while no suppression effect was observed from dSC iRed/fET without chloroquine (Figure 25).

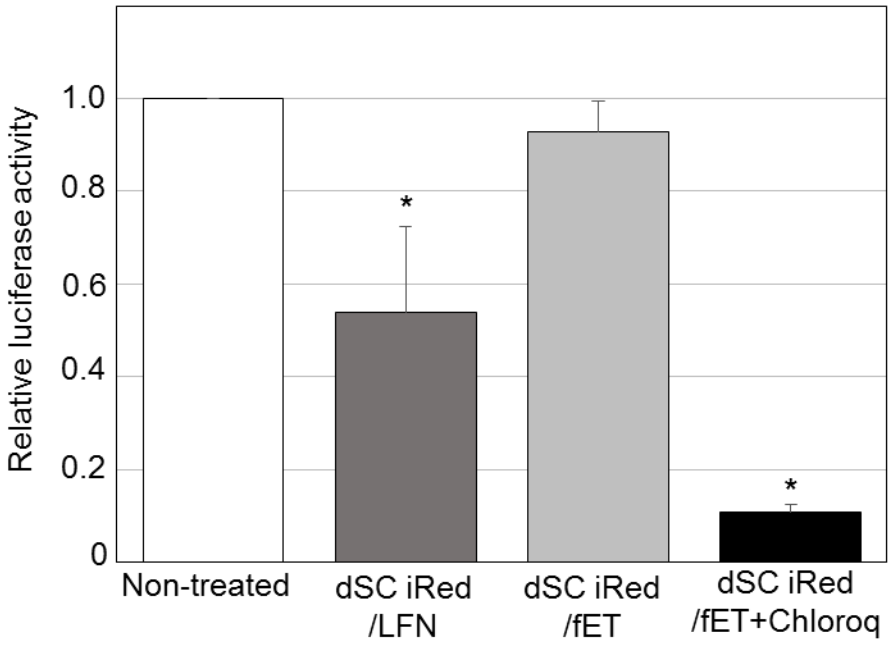

Figure 25. Effect of iRed/fET on luciferase activity of cells in the presence of chloroquine. Luciferase activity of B16F1-Luc cells was measured after 24 h of fET (0.34 mA/cm^2, 15 min) with Chloroquine. LFN/dSC iRed used as positive control. The concentration of chloroquine was 100 μM. Data were obtained from three separate experiments and expressed as mean mean ± SD. *p<0.05. ***Sci. Technol. Avd. Mater. 2016, 17, 554-562, Figure 5.***

Additionally, chloroquine also increased the suppression effect of dSC iRed/lFN lipoplex (Figure 26). But, the RNAi effect obtained from dSC iRed/fET with chloroquine was more potent than that of the dSC iRed/LFN lipoplex even with chloroquine. This result indicates that, in the presence of endosomal escaping agent, fET based delivery of dSC iRed is more effective than that of the lipoplex systems.

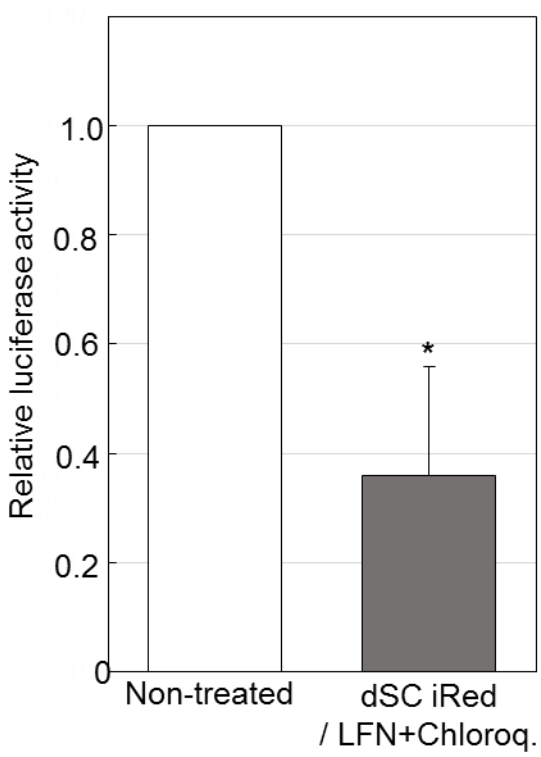

Figure 26. Effect of chloroquine on transfection of iRed/LFN lipoplex
Luciferase activity of cells expressing luciferase was measured 24 h after transfection with LFN/iRed lipoplex. Concentration of chloroquine was 100 μM. Data were obtained by three separate experiments, and are expressed as mean ± SD. Statistical analysis was performed using Student's t-test. **p*-values < 0.05 was considered to be significant. **p*<0.05 vs non-treated. ***Sci. Technol. Avd. Mater. 2016, 17, 554-562, Supplemental Figure 2.***

2-5 Effect of RNAi provided by dSC iRed/ fET on phenotypes of pathological adipocyte

Adipokines are physiologically active cytokines secreted from adipocytes [63]. Resistin is one of the key adipokine associated with obesity which is known as one cause of metabolic syndrome. Resistin contributes to the lipid accumulation during adipocyte maturations of 3T3-L1 cells [60]. Transfection of anti-resistin siRNA by commercially available transfection reagent is reported to reduce lipid accumulation during adipocyte maturation [60]. Thus, RNAi of resistin gene would be useful for prevention of obesity. To study the possible use of dSC iRed/fET in RNAi therapy, effect of fET with dSC iRed encoding anti-resistin shRNA on adipocyte maturation of 3T3-L1 cells was evaluated. In the maturation process, 3T3-L1 cells can accumulate lipid droplet depending on the maturation process. First, the maturation dependent lipid accumulation in 3T3-L1 cells was monitored. It was found that after addition of designated maturation medium, cells started to accumulate lipid droplets and the amount of lipid accumulation was significantly increased with time of incubation (Figure 27- a & b).

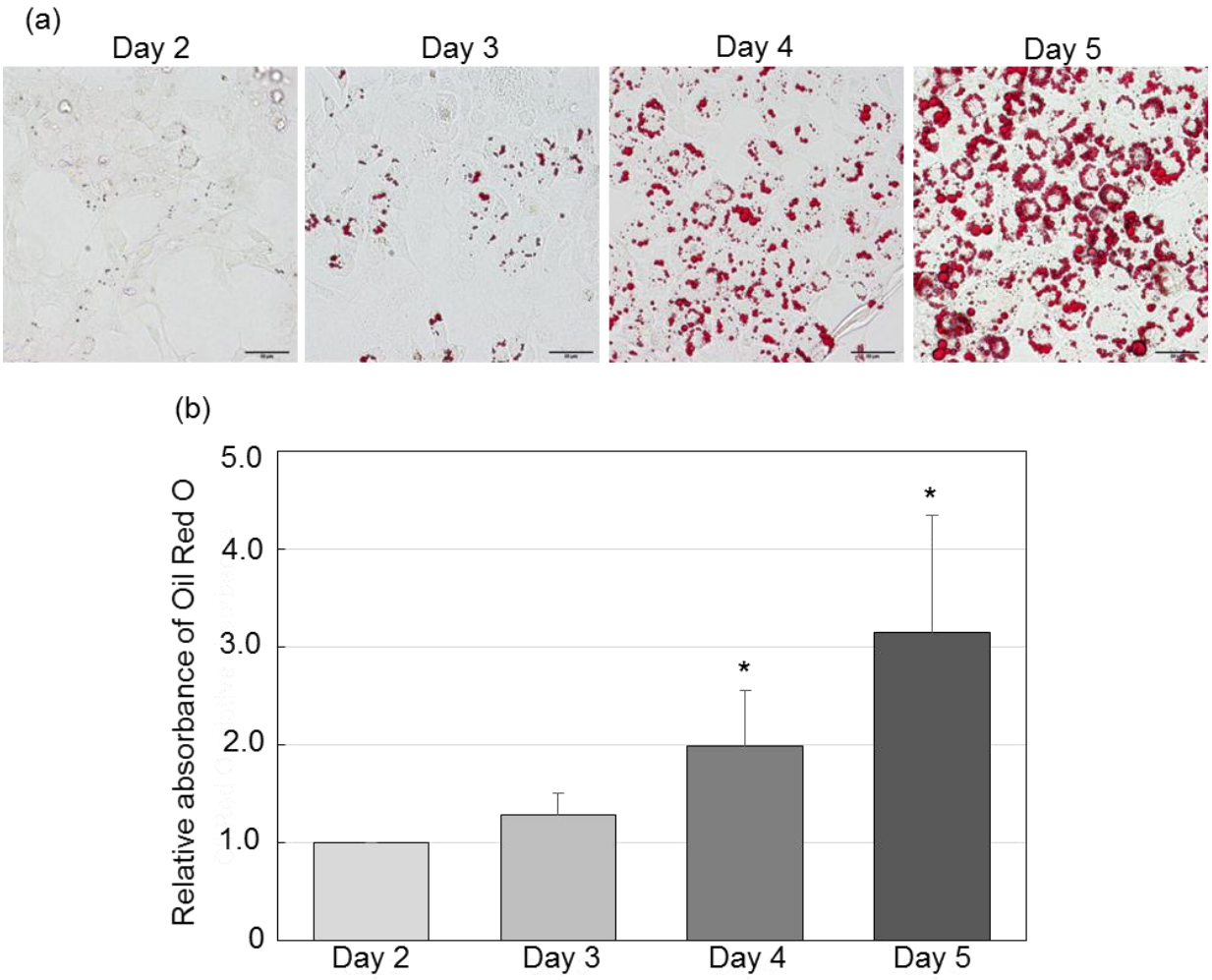

Figure 27. Maturation dependent accumulation of lipid droplet in 3T3-L1 cells. After induction of maturation, the cells were fixed and stained with Oil Red O. (a) Microscopy images of 3T3-L1 adipocytes stained with Oil Red O on day 2 - day 4. The scale bars indicate 50 μm. (b) Relative absorbance of Oil Red O dye extracted from 3T3-L1 adipocytes after Oil Red O staining. Data were obtained by three separate experiments, and are expressed as mean ± SD. *p<0.05 vs non-treated. ***Sci. Technol. Avd. Mater. 2016, 17, 554-562, Supplemental Figure 3.***

Next, the fET of 3T3-L1 cells with dSC iRed against resistin after induction of adipocyte maturation was examined. The lipid droplet accumulated in the cells at day 4 after induction of maturation was significantly reduced by fET with iRed in the presence of chloroquine (Figure 28-a). Additionally, the absorbance of Oil red O, which is an indicator of intracellular lipid accumulation, was suppressed 35 % by iRed/fET with chloroquine (Figure. 28-b). Although the suppression level of Oil red O absorbance by fET was almost the same as LFN with chloroquine (Figure. 28-b), reduction of Oil red O staining by fET seems to be more

homogeneous than that with LFN (Figure. 28-a). Thus, these results mean that fET of iRed against registin with chloroquine would be a useful method for regulation of lipid accumulation during adipocyte maturation.

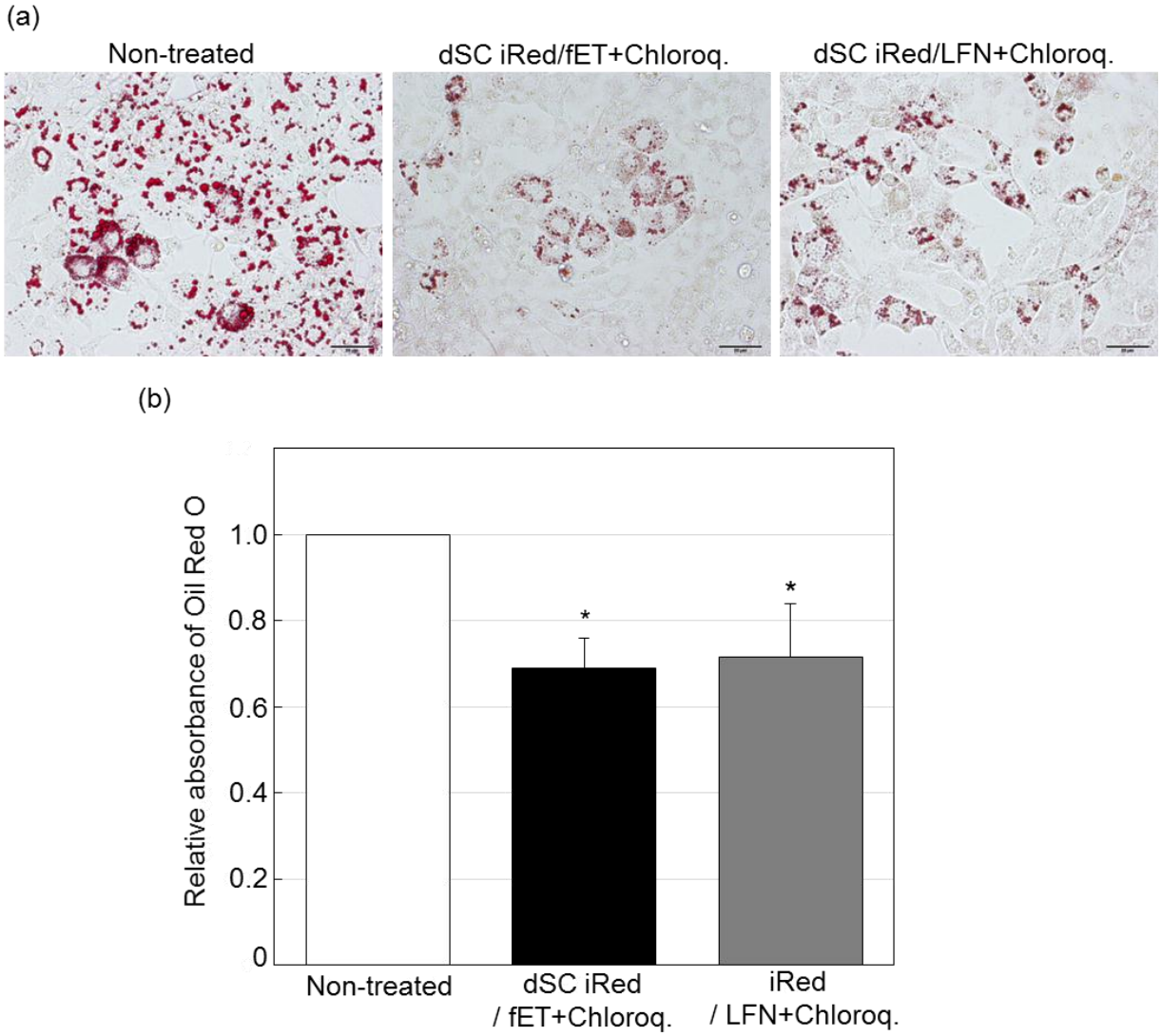

Figure 28. Effect of fET mediated transfection of dSC iRed encoding resisting on lipid accumulation in 3T3-L1 adipocytes in the presence of chloroquine. After transfection of dSC iRed against resistin by fET in the presence of chloroquine, 3T3-L1 adipocytes were fixed and stained with Oil Red O. (a) Microscopy images of cells stained with Oil Red O. Scale bars indicate 50 μm. (b) Relative absorbance of Oil Red O dye extracted from cells after Oil Red O staining. Data were obtained by three separate experiments, and are expressed as mean ± SD. *p<0.05 versus non-treated. ***Sci. Technol. Avd. Mater. 2016, 17, 554-562, Figure 6.***

Additionally, the effect of anti-resistin dSC iRed/fET without chloroquine on adipocyte maturation was also examined. As a result, no suppression effect on lipid accumulation was observed (Figure. 29- a & b). This result is consistent with anti-luciferase dSC iRed/fET in the absence of chloroquine.

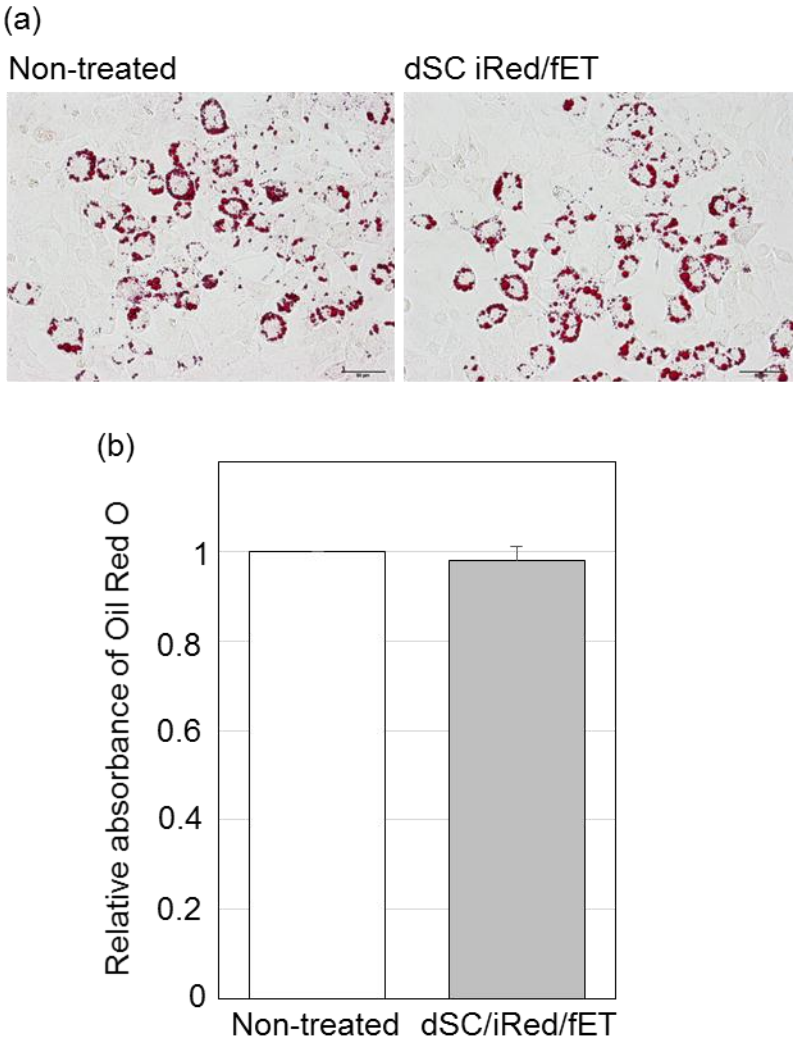

Figure 29. Effect of fET mediated transfection of dSC iRed encoding resisting on lipid accumulation in 3T3-L1 adipocytes without chloroquine.

After transfection of dSC iRed against resistin by fET, 3T3-L1 adipocytes were fixed and stained with Oil Red O. (a) Microscopy images of cells stained with Oil Red O. Scale bars indicate 50 μm. (b) Relative absorbance of Oil Red O dye extracted from cells after Oil Red O staining. Data were obtained by three separate experiments, and are expressed as mean ± SD. **p*<0.05 versus non-treated. ***Sci. Technol. Avd. Mater. 2016, 17, 554-562, Supplemental Figure 4.***

2-6 Evaluation of intracellular fate of dSc iRed internalized by fET

To evaluate the intracellular fate of dSC iRed in 3T3-L1 cells, the intracellular trafficking of FITC-labeled dSC iRed was examined.

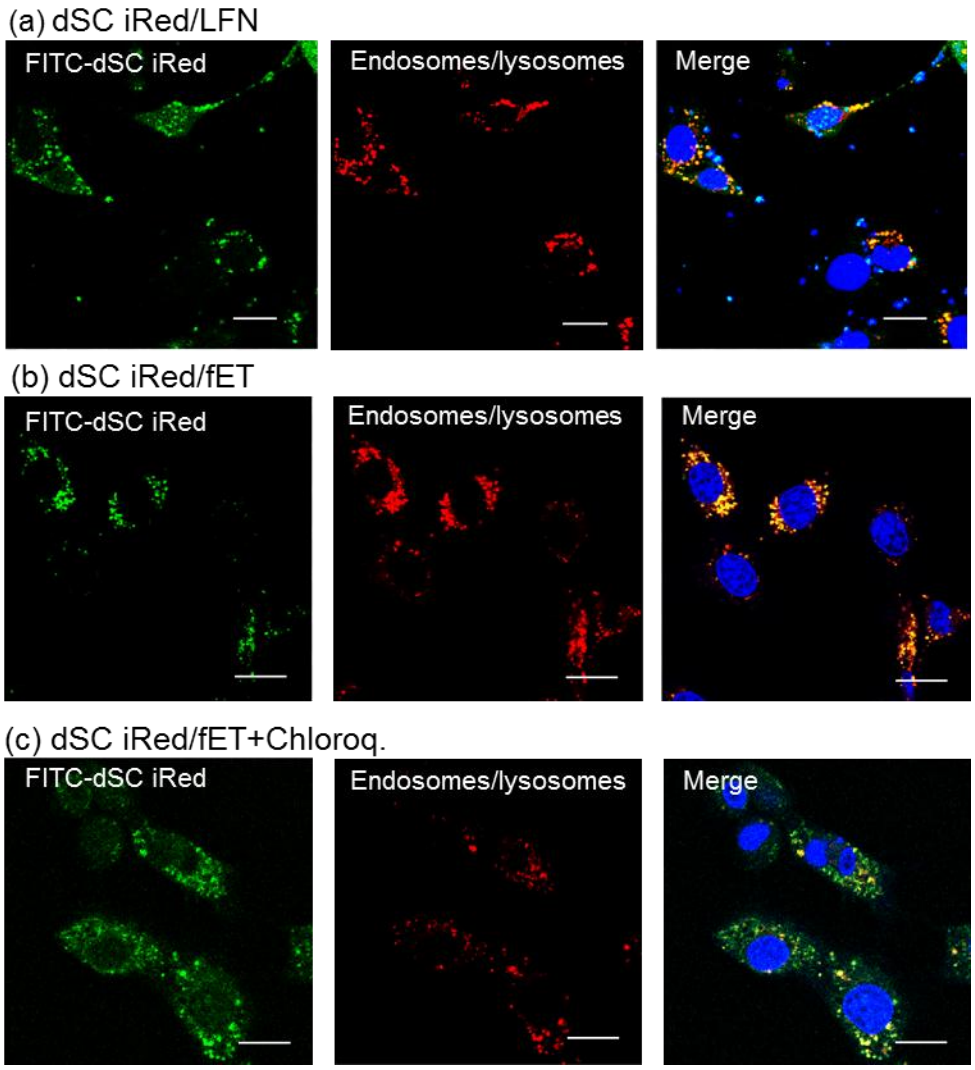

Figure 30. CLSM images of intracellular fate of dSC iRed.
Cells were treated with FITC-labeled dSC iRed/lipoplex (a) or fET (0.34 mA/cm^2 for 15 min) with or without chloroquine in the presence of FITC-labeled dSC iRed (b, c). After the incubation for 3 h, cells were observed by a confocal laser scanning microscope. Intracellular distribution of FITC-labeled dSC (green) and endosomes/lysosomes stained with lyso tracker (red) were shown as individual images, respectively. In the merged images, nuclei were stained with Hoechst 33342 (blue) to recognize intracellular positions of FITC-labeled dSC and endosome/lysosomes. Scale bars indicate 20 μm. ***Sci. Technol. Avd. Mater. 2016, 17, 554-562, Figure 7.***

Similar to the result of Figure 23, it was found that green dots of FITC-labeled iRed was co-localized with red dots of endosomes stained with Lyso Tracker red without chloroquine (Figure. 30-b). On the other hand, green fluorescence signals of FITC-labeled iRed were widely distributed in cells when fET was performed in the presence of chloroquine (Figure. 30-c). These results indicate that the endosomal escape of dSC iRed was difficult even after fET without chloroquine.

3 Discussion

Intelligent shRNA expression device (iRed) is a synthetic 4'-thiol DNA construct. It acts as template for generating shRNA in cells. Minimal-size and higher stability of iRed make it superior than conventional RNAi tools. However, shRNA expression from iRed is needed to induce RNAi effect. Nucleus is the intracellular site of iRed for generating shRNA. After cellular uptake and endosomal escape of iRed into cytoplasm, it needs to travel relatively long distance through the mesh of cytoskeleton to reach the nuclear membrane. Once at the nuclear membrane, iRed either waits for cell division or transports through the nuclear pore complex to enter into the nucleus and transcribe into shRNA. Then, shRNA exports from nucleus to cytoplasm to induce RNAi effect (Figure 19). Non-viral cationic nanocarriers are general option for delivery of iRed into cells. However, cationic group of nanocarriers interacts with cellular component via electrostatic interaction to induce toxicity or non-specific RNAi effect. Therefore, carrier independent delivery technology would be effective for intracellular delivery of iRed. Since fET induces rapid and homogeneous delivery of FNAs into the cells found in chapter I, fET was applied for intracellular delivery of dSC iRed.

After transfection, dSc iRed/LFN lipoplex showed significant RNAi effect although the effect was nearly similar than that of siRNA/LFN lipoplex (Figures 21 & 6). This result means that shRNAs were produced from dSC iRed. On the other hand, RNAi effect was not found from dSC iRed/fET. To know why dSC iRed/fET showed no RNAi, cellular uptake of fluorescent-labeled siRNA was examined. The result that fluorescence intensity of the lysate was significantly higher than LFN lipoplexes indicates that fET-based delivery of functional nucleic acids is faster and effective than LFN lipoplex in short incubation period such as 3 h.

In chapter I, it was also found that fET induced efficient cellular uptake of functional nucleic acids siRNA and ISMB (Figures 6 & 9). The differences between siRNA/ISMB and dSC iRed were expressed by their molecular size. The molecular weights of ISMB, siRNA and dSC iRed are 11,200, 14,000, and 225,000 respectively. Thus, the significantly higher molecular size of dSC iRed than ISMB or siRNA may be a factor for contributing inadequate endosomal escape of dSC iRed. The result of intracellular trafficking for different sized molecules such as FITC-dextran 10,000 and FITC-dextran 70,000 after 24 h of fET showed that FITC-dextran 70,000 fluorescence remains in cell as dots not widely distributed in the cell like FITC-dextran 10,000, suggesting that endosomal escape of materials taken up by fET depends on their molecular sizes. The properties of endosomes after fET seem to be leaky to a certain molecular weight. That's why relatively lower molecular sized molecules such as siRNA and ISMB may leak out from endosomes to cytoplasm and associate with their targets. On the other hand, the significant higher molecular size of iRed makes it difficult to leak out from endosomes and remains in the endosome even after fET. In Figure 23, signals of lyso tracker red remained very weak. Lyso tracker red might be leaked out from endosomes due to the leaky property of endosomes induced by fET. Moreover, long period of incubation after fET might attenuate the acidification of endosomes, resulting in the weak signals of lyso tracker red. Therefore, after fET based transfection, the endosomal scape of dSc iRed is thought to be difficult due to its huge molecular

size. Use of lysosomotropic agent is an approach to enhance endosomal escape of materials internalized by endocytosis. Chloroquine, which is a hydrophobic weak base is well known as an anti-malaria drug, and also acts as lysosomotropic agent. [64, 61, 62]. Chloroquine that enters into the endosome is protonated by the acidic environment of endosome, following destabilization of the endosomal membrane. To enhance endosomal escape of macromolecules, 50 μM -150 μM chloroquine is usually used [61, 62]. Therefore, the endosomal escape barrier of iRed after fET was overcome by using chloroquine (100 μM) in this study. Interestingly, transfection of dSC iRed following fET in the presence of chloroquine significantly suppressed luciferase expression and this RNAi effect was higher than dSC iRed/LFN lipoplex with or without chloroquine (Figures 25 & 26). Although it is known that chloroquine shows cytotoxicity, the RNAi effect from dSC iRed/LFN lipoplex without chloroquine remained nearly similar to dSC iRed/LFN lipoplex with chloroquine (Figures 25 & 26). This result suggests that potent RNAi effect obtained from transfection of dSC iRed after fET with chloroquine is caused by effective cytoplasmic delivery of dSC iRed, not by the cytotoxicity. The dSc iRed delivered with cationic nanoparticles must be released from lipoplex to exert its effect, while fET delivered naked dSC iRed. Due to the difficulties for dSC iRed to release from lipoplex or non-specific binding of cationic groups with cellular component, few amounts of dSc iRed may enter into the nucleus. Additionally, cationic lipoplex seems to interact with shRNA produced from dSC iRed to prevent RNAi effect. On the other hand, it has been reported that naked FNAs can bind indirectly to the microtubules in assistance with adaptor proteins to travel towards nucleus [65]. After improvement of endosomal escape of naked dSC iRed taken up by fET, it may be efficiently entered into the nucleus. Thus, RNAi effect obtained from fET/dSC iRed was higher than that of LFN/dSc iRed. Based on this result, fET would be a useful technology to deliver functional nucleic acids without affecting their activity. Thus, a combination of dSC iRed with fET in the presence of endosomal escaping agent without cytotoxicity could be applied for RNAi therapy against various diseases.

Obesity is one of the main cause of metabolic syndrome. Resistin is an adipose tissue secreted adipokine which is associated with adipocyte maturation as well as for the development of obesity [66]. Thus, the regulation of resistin gene would be useful for preventing of obesity. Here, fET of dSc iRed encoding anti-resistin shRNA in the presence of chloroquine was examined on adipocyte maturation. From our result, lipid accumulation was suppressed 35% by dSC iRed /fET with chloroquine (Figure 28-a & b). This suppression level remained almost same as that for LFN/dSC iRed. But the suppression pattern obtained from fET appeared to be more homogeneous than that observed from LFN. Besides resistin, some other adipokines are also found to be involved in adipocyte maturation, thereby the suppression of lipid accumulation was not so potent like luciferase activity suppression.

The analysis of the intracellular trafficking of FITC-labeled dSc iRed in 3T3-L1 cells suggests that endosomal escape of dSc iRed was difficult even after fET without chloroquine. These findings are consistent with the effect of anti-luciferase iRed on luciferase activity in the presence or absence of chloroquine in B16F1-Luc cells. Thus the effects of molecular size on fET mediated cytoplasmic delivery may be a common phenomenon in both B16F1 cells and 3T3-L1 cells. Upon using lysosomotropic agent

choloroquine, the effect of molecular size was improved in this study. As such, dSC iRed/fET with chloroquine showed a significantly higher RNAi effect than dSC iRed/LFN lipoplexes. Furthermore, fET of dSC iRed carrying shRNA against resistin in the presence of chloroquine suppressed lipid accumulation that occurs during adipocyte maturation. Together, these results indicate that a combination of dSC iRed with fET is a useful method for effective regulation of target gene expression.

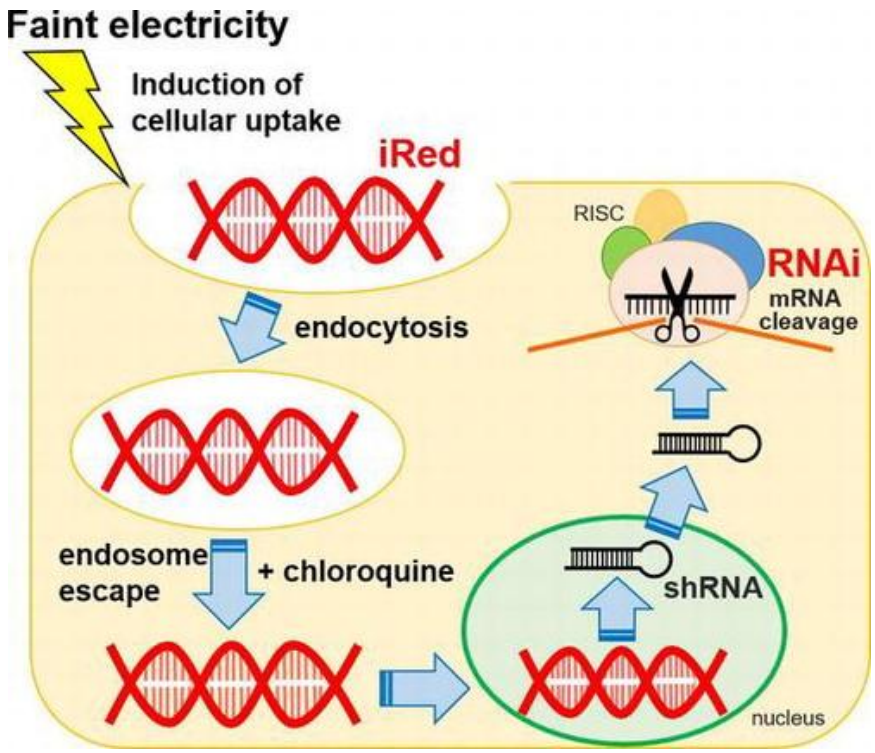

Figure 31. Graphical summary of chapter II. After fET mediated cellular uptake, iRed remains in endosome. Chloroquine induces endosomal escape of iRed into cytoplasm. In assistance with cellular function, iRed enters into the nucleus and transcribes into shRNA. Then, shRNA exports into cytoplasm and showed RNAi effect.

Sci. Technol. Avd. Mater. 2016, 17, 554-562, Graphical abstract.

Conclusion

The present study concluded that faint electric treatment (fET) can induce rapid cellular uptake and homogenous delivery of functional nucleic acids into cell cytoplasm without inducing electricity based cytotoxicity. The cellular uptake pathway activated by fET was endocytosis. fET mediated alteration of membrane potential via activation of cationic ion channels would activate cellular uptake pathway. Furthermore, fET mediated delivery of a novel functional nucleic acid iRed encoding resistin in the presence of endosomal escaping agent showed significant regulation of lipid accumulation in adipocytes for application to obesity therapy. Thus, fET could be useful for effective and safe delivery of functional nucleic acids such as siRNA, miRNA and antisense oligonucleotides into the cytoplasm of cells for effective regulation of target genes.

Acknowledgements

First and foremost, I would like to express my sincere gratitude to Professor *Kentaro Kogure*. If I look back three years, I came from Bangladesh for his great motivations. He taught and supervised me with immense knowledge, joy and enthusiasm. Besides academic activities, he introduced my life in Kyoto and also provided financial support.

I am thankful to Dr. *Susumu Hama* for his great supervision and continued supports after leaving Professor *Kogure* from Kyoto Pharmaceutical University. He introduced me with diverse fields of drug delivery systems. I appreciate all his supports regarding experimental protocols, data analysis, and preparation of thesis.

I am lucky to have another supportive Professor *Hiroyuki Saito* in my study. I express my sincere thanks to Professor *Saito* for his continued supports, motivations and kindness in every aspects of my study and extracurricular activities.

I am thankful to Dr. *Takashi Ohgita* for all of his technical supports in the laboratory.

I would like to acknowledge Professor *Hiroyuki Asanuma*, Dr. *Hiromu Kashida*, Department of Molecular Design and Engineering, Nagoya University, for providing in-stem molecular beacon (ISMB), Professor *Noriaki Minakawa* and Dr. *Noriko Tarashima*, Graduate School of Pharmaceutical Science, Tokushima University, for providing intelligent shRNA expression device (iRed) used in this study.

I am thankful to all undergraduate and graduate students, staff in the Laboratory of Biophysical Chemistry for their unconditional supports during the study period.

I express my gratitude and thanks to 'Tokyo Biochemical Research Foundation' and 'Kyoto Pharmaceutical University' for providing me scholarship during the study period.

Lastly, I am thankful to my lovely wife *Anowara Khatun* for her infinitive supports and motivations regarding my study and life in this lonely planet.

Hasan Mohammad Mahadi
Department of Biophysical Chemistry
Kyoto Pharmaceutical University, Japan

References

1) J. L. Rudolph. The delivery of therapeutic oligonucleotides. *Nucleic Acid Res.* 2016, 44, 6518-6548.
2) S. Kannan and G. N. Jaideep. Therapeutic nucleic acids: current clinical status. *Br. J. Clin. Pharmacol.* 2016, 82, 659-972.
3) J. H. Charles, C. Chin-Kaung, R. Anitha, R. Snehal and P. A. Blaine. Overcoming non-viral gene delivery barriers: perspective and future. *Mol. Pharm*. 2013, 10, 4082-4098.
4) D. Nathalie and C. A. Stein. Antisense oligonucleotides: Basic concepts and mechanisms. *Mol. Cancer Ther.* 2002, 5, 347-355.
5) K. E. Lundin, O. Gissberg and C. I. Smith. Oligonucleotide therapeutics: The past and present. *Hum. Gene Ther.* 2015, 26, 475-485.
6) C. Chen, Z. Yang and X. Tang. Chemical modification of nucleic acids drug and their delivery systems for gene based therapy. *Med. Res. Rev*. 2018, 1-41.
7) W. Jie, L. Ze, W. Guillaume and J. L. Au. Delivery of siRNA therapeutics: Barriers and carriers. *AAPS J.* 2010, 12, 492-503.
8) A. Khvorova and J. K. Watts. Chemical evolution of oligonucleotide therapies of clinical utilities. *Nat. Biotechnol*. 2017, 35, 238-248.
9) I. A. Khalil, K. Kogure, H. Akita and H. Harashima. Uptake pathway and subsequent intracellular trafficking in non-viral gene delivery. *Pharmacol. Rev*. 2006, 58, 32-45.
10) V. K. Amir, S. Marije, S. Gert and H. Hidde. Endosomal escape pathway for delivery of biologicals. *J. Control. Release* 2011, 151, 220-228.
11) J. Gilleron, W. Querbes, A. Zeigerer, A. Borodovsky, G. Marsico, U. Schubert, K. Manygoats, S. Seifert, C. Andree, M. Stöter, H. Epstein-Barash, L. Zhang, V. Koteliansky, K. Fitzgerald, E. Fava1, M. Bickle, Y. Kalaidzidis, A. Akinc, M. Maier and M. Zerial. Image-based analysis of lipid nanoparticle–mediated siRNA delivery intracellular trafficking and endosomal escape. *Nat. Biotechnol*. 2013, 31, 638-646.
12) Leo Chou, Kevin. Ming and Warren Chan. Strategies for the intracellular delivery of nanoparticles, *Chem. Soc. Rev*. 2011, 40, 233-245.
13) L. Xu, and T. Anchordoquy. Drug delivery trends in clinical trials and translational medicine: Challenges and opportunities in the delivery of nucleic acid based therapeutics. *J. Pharm. Sci.* 2011, 100, 38-52.
14) M. P. Stewart, A. Sharei, X. Ding, G. Sahay, R. Langer and K. F. Jensen. *In vivo* and *ex vivo* strategies for intracellular delivery. *Nature* 2016, 538, 183-192.
15) M. A. Mintzer and E. E. Simanek. Nonviral vectors for gene delivery. *Chem. Rev*. 2009, 109, 259-302.
16) N. Nayerossadat, T. Maedeh and P. A. Ali. Viral and nonviral delivery system for gene delivery. *Adv. Biomed. Res.* 2012, 1, 27.
17) G. Sahay, D. Alakhova and A. Kabanov. Endocytosis of nanomedicines. *J. Control. Release* 2010, 145, 182-195.
18) L. Hongtao, S. Zhang, B. Wang, S. Cui and J. Yan. Toxicity of cationic lipids and polymers in gene delivery. *J. Control. Release* 2006, 114, 100-109.

19) L. Jin, X. Zeng, M. Liu, Y. Deng and H. Nongyue. Current progress in gene delivery technology based on clinical methods and nonocarriers. *Theranostics* 2014, 4, 240-255.
20) J. Agarwal, A. Walsh and R. Lee. Multimodal strategies for resuscitating injured cells. *Ann. NY Acad. Sci.* 2005, 1066, 295-309.
21) C. E. Thomas, A. Ehrhardt and M. A. Kay. Progress and problems with the use of viral vectors for gene therapy. *Nature* 2003, 4, 346-358.
22) C.M. Schoellhammer, D. Blankschtein, R. Langer. Skin permeabilization for transdermal drug delivery: recent advances and future prospects. *Expert Opin. Drug Deliv*. 2014. 11, 393-407.
23) T.W. Wong. Electrical, magnetic photomechanical and cavitation waves to overcome skin barrier for transdermal drug delivery. *J. Control. Release.* 2014, 193, 257-269.
24) T. Gratieri, I. Aiberti, M. Lapteva, Y.N. Kalia, Next generation intra and transdermal therapeutic system: using non- and minimally invasive technologies to increase drug delivery into and across the skin. *Eur. J. Pharm. Sci*. 2013. 50, 609-622.
25) N. Dixit, V. Bali, S. Baboota, A. Ahuja and J. Ali. Iontophoresis- an approach for control drug delivery: a review. *Curr. Drug Deliv*. 2007, 4, 1-10.
26) K. Kigasawa, K. Kajimoto, S. Hama, K. Kanamura and K. Kogure. Noninvasive delivery of siRNA into the epidermis by iontophoresis using an atopic dermatitis-like model rat. *Int. J. Pharm.* 2010, 383, 157-160.
27) Kigasawa K, Kajimoto K, Nakamura T, Hama S, Kanamura K, Harashima H, Kogure K. Noninvasive and efficient transdermal delivery of CpG-oligodeoxynucleotide for cancer immunotherapy. *J. Control. Release* 150, 256-265.
28) Kajimoto K, Yamamoto M, Watanabe M, Kigasawa K, Kanamura K, Harashima H, Kogure K. Noninvasive and persistent transfollicular drug delivery system using a combination of liposomes and iontophoresis. *Int. J. Pharm.* 2011, 403, 57-65.
29) S. Hama, Y. Kimura, A. Mikami, K. Shiota, M. Toyoda, A. Tamura, Y. Nagasaki, K. Kanamura, K. Kajimoto and K. Kogure. Electric stimulus opens intracellular space in skin. *J. Biol. Chem.* 2014, 289, 2450-2456.
30) S. Sundelacruz, M. Levin and D. L. Kaplan. Role of membrane potential in regulation of cell proliferation and differentiation. *Stem Cell Rev*. 2009, 5, 231-246.
31) X. Wu, B. D. McNeil, J. Xu, J. Fan, L. Xue, E. Melicoff, R. Adachi, L. Bai and L. Wu. Ca^{2+} and calmodulin initiate all forms of endocytosis during depolarization at a nerve terminal. *Nat. Neurosci.* 2009, 12, 1003-1010.
32) H. Kashida, T. Osawa, K. Morimoto, Y. Kamiya, H. Asanuma. Molecular design of Cy3 derivative for highly sensitive in-stem molecular beacon and its application to the wash-free FISH. *Bioorg. Med. Chem.* 2015, 23, 1758-1762.
33) S. Tran, A. Puhar, M. Ngo-Camus, and N. Ramarao. Trypan blue dye enters viable cells incubated with the pore-forming toxin HlyII of Bacillus cereus. *PLoS One* 2011, 6, e22876.
34) M. Koivusalo, C. Walch, H. Hayashi, C. C. Scott, M. Kim, T. Alexander, N Touret, K. M. Hahn and S. Grinstein. Amiloride inhibits macropinocytosis by lowering submembranous pH and preventing Rac1 and Cdc42 signaling. *J. Cell Biol.* 2010, 22, 547-563.

35) J. E. Heuser and R. G. W. Anderson. Hypertonic media inhibit receptor mediated endocytosis by blocking clathrin-coated pit formation. *J. Cell Biol.* 1989, 108, 389-400.
36) J. Rejman, A. Bragonzi and M. Conese. Role of clathrin and caveolae-mediated endocytosis in gene transfer mediated by lipo and polyplex. *Mol. Ther.* 2005, 12, 468-474.
37) K.R. Konrad and R. Hedrich. The use of voltage-sensitive dyes to monitor signal induced changes in membrane potential-ABA triggered membrane depolarization in guard cells. *Plant J*. 2008, 55, 161-173.
38) A. Singh, M. Hildebrand, E. Garcia and T. Snutch. The transient receptor potential channel antagonist SKF96365 is a potent blocker of low-voltage-activated T-type calcium channel. *Br. J. Pharmacol*. 2010, 160, 1464-1475.
39) A. Mitsueda, Y. Shimatani Y, M. Ito, T. Ohgita, A. Yamada, S. Hama, A. Gräslund, S. Lindberg, U. Langel, H. Harashima, I. Nakase, S. Futaki and K. Kogure. Development of a novel nanoparticle by dual modification with the pluripotential cell-penetrating peptide PepFect6 for cellular uptake, endosomal escape, and decondensation of siRNA core complex. *Biopolymers* 2013, 100, 698-704.
40) K. J. Stacey, I. L. Ross and D. A. Hume. Electroporation and DNA-dependent cell death in murine macrophages. *Immunol. Cell. Biol*. 1999, 71, 75-85.
41) C. C. Chang, M. Wu and F. Yuan. Role of specific endocytic pathways in electrotransfection of cells. *Mol. Ther. Methods Clin. Dev*. 2014, 1, 14058.
42) M. Elsabahy, A. Nazarali and M. Foldvari. Non-viral nucleic acid delivery: Key challenges and future directions. *Curr. Drug Deliv*. 2011, 8, 235-244.
43) H. Y. Xue, S. Liu and H. L. Wong. Nanotoxicity: a key obstacle to clinical transfection of siRNA based nanomedicine. *Nanomedicine* 2014, 9, 295-312.
44) A. A. Chen, A. M. Derfus, S. R. Khetani and S. N. Bhatia. Quantum dots to monitor RNAi delivery and improve gene silencing. *Nucleic Acid Res*. 2005, 33, e 190.
45) L. C. Thuc, Y. Teshima, N. Takahashi, S. Nishio, A. Fukui, O. Kume, S. Saito, M. Nakagawa and T. Saikawa. Inhibition of Na^+-H^+ exchange as a mechanism of rapid cardioprotection by resveratrol. *Br. J. Pharmacol*. 2012, 166, 1724-1755.
46) B. Zhang, J. S. Naik, N. L. Jernigan, B. R. Walker and T. C. Resta. Reduced membrane cholesterol limits endothelial Ca^{2+} entry after chronic hypoxia. *Am. J. Physiol. Heart Circ. Physiol*. 2017, 312, 1176-1184.
47) T. Brauner, D. F. Hulser and R. J. Strasser. Comparative measurement of membrane potentials with microelectrodes and voltage sensitive dyes. *Biochim. Biophys. Acta* 1984, 771, 208-216.
48) J. Zheng. Molecular mechanism of TRP channels. *Compr. Physiol*. 2013, 3, 221-242.
49) D. E. Clapham. TRP channels as cellular sensors. *Nature* 2003, 426, 517-524.
50) C. Callies, J. Fels, I. Liashkovich, K. Kliche, P. Jeggle, K. Kusche and H. Oberleithner. Membrane potential depolarization decreases the stiffness of vascular endothelial cells. *J. Cell Sci*. 2011, 124, 1936-1942.
51) F. Waheed, P. Speight, G. Kawai, Q. Dan, A. Kapus and K. Szaszi. Extracellular signal regulated kinase and GEF-H1 mediate depolarization-induced Rho activation and paracellular permeability increase. *Am. J. Physiol. Cell Physiol.* 2010, 298, 1376-1387.
52) B. Qualmann and H. Mellor. Regulation of endocytic traffic by Rho GTPase. *Biochem. J.* 371, 233-241.

53) H. Peacock, A. Kannan, and P.A. Beal PA. Chemical modification of siRNA bases to probe and enhance RNA interference. *J. Org. Chem.* 2011, 76, 7295–7300.
54) H. Shirota, D. Tross, and D.M. Klinman. CpG oligonucleotides as cancer vaccine adjuvants. *Vaccines* 2015, 3, 390–407.
55) N. Tarashima, H. Ando, T. Kojima, N. Kinjo, Y. Hashimoto, K. Furukawa, T. Ishida and N. Minakawa. Gene Silencing Using 4'-thioDNA as an artificial template to synthesize short hairpin RNA without inducing a detectable innate immune response. *Mol. Ther. Nucleic Acids* 2016, 5, e274.
56) Y. W. Won, D. A. Bull and S. W. Kim. Functional polymers of gene delivery for treatment of myocardial infarct. *J. Control. Release* 2014, 195, 110–119.
57) B. Ozpolat, A. K. Sood and G. Lopez-Berestein. Liposomal siRNA nanocarriers for cancer therapy. *Adv. Drug Deliv. Rev.* 2014, 66, 110–116.
58) S. Hama, H. Akita, S. Iida, H. Miguguchi and H. Harashima. Quantitative and mechanism-based investigation of post-nuclear delivery events between adenovirus and lipoplex. *Nucleic Acids Res*. 2007, 35, 1533–1543.
59) N. Inoue, A. Shionoya, N. Minakawa, A. Kawakami, N. Ojawa and A. Matsuda . Amplification of 4'-ThioDNA in the presence of 4'-Thio-dTTP and 4'-Thio-dCTP, and 4'-ThioDNA-directed transcription in vitro and in mammalian cells. *J. Am. Chem. Soc*. 2007, 129, 15424–15425.
60) Y. Ikeda, H. Tsuchiya, S. Hama, K. Kajimoto and K. Kogure. Resistin affects lipid metabolism during adipocyte maturation of 3T3-L1 cells. *FEBS J.* 2013, 280, 5884–5895.
61) A. El-Sayed, I.A. Khalil, K. Kogure, S. Futaki and H. Harashima. Octaarginine- and octalysine-modified nanoparticles have different modes of endosomal escape. *J. Biol. Chem.* 2008, 283, 23450–2346.
62) C. Cordier, F. Boutimah, M. Bourdeloux, F. Dupui, E. Met, P. Alberti, F. Loll, G. Chassing, F. Burlina, T. E. Saison. Delivery of antisense peptide nucleic acids to cells by conjugation with small arginine-rich cell-penetrating peptide (R/W) 9. *PLoS One*. 2014, 9, e104999.
63) G. Fantuzzi. Adipose tissue, adipokines, and inflamation. *J. Allergy Clin. Immunol*. 2005, 115, 911-920.
64) A. Anez, M. Moscoso, C. Garnica and C. Ascaso. Evaluation of the paediatric dose of chloroquine in the treatment of *Plasmodium vivax* malaria. *Malar. J.* 2016, 15, 371.
65) R. Zhou, R. C. Griger and D. A. Dean. Intracellular trafficking of nucleic acids. *Expert Opin. Drug Deliv*. 2004, 1, 127-140.
66) K. Srikanthan, A. Feyh, H. Visweshwar, J. I. Shapiro and K. Shodhi. Systematic review of metabolic syndrome biomarkers: A panel for early detection, management, and risk stratification in the West Virginian population. *Int. J. Med. Sci*. 2016, 13, 25-38.